university of groningen

faculty of science and engineering

Synchronization in electrical circuits with memristive elements

Master's Project Applied Mathematics

November 2020

Student: Vasiliki Vamvaka

First supervisor: Dr.ir. B. Besselink

Second assessor: Dr. A. E. Sterk

Abstract

This thesis presents and analyzes the dynamics of electrical circuits with memristive components. Memristive devices add a new dimension for modelling innovative circuits and systems in a wide range of applications, such as neural networks, storage devices and neuromorphic circuits- in which the memristive devices can act as artificial synapses. The main property of memristive devices is the non-volatile memory, which makes memristors ideal as potential building blocks for neuromorphic computer architectures. Neuromorphic computing is a new technology inspired by the human brain, with great potential to enable information processing at very low cost, using electronic devices that imitate the electrical behaviour of biological neural networks. First, we study synchronization in networks consisting of memristors and capacitors. Subsequently, electrical circuit models of (biological) neurons coupled via memristors are considered. Accordingly, the system of differential equations that simulate the well-known FitzHugh-Nagumo (FHN) neuron model is adopted, in order to derive a sufficient condition on the coupling coefficient to guarantee synchronization of FHN neuron-memristor network, by using Lyapunov stability theory. Finally, simulation results illustrate the synchronization phenomena of the proposed electrical circuits.

Contents

1 Introduction

1.1 Background

Over the past few decades, the exponential growth of computing technologies has reshaped almost every aspect of society, from how people communicate and work to understanding the world around us and the universe beyond. Nonetheless, computing systems, such as computers and smartphones, as well as the Internet, consume large amounts of energy. In addition, large amounts of energy are consumed by data centers, which are physical facilities where computing equipment is concentrated for the purpose of storing digital data. This motivates us to always seek for alternatives to make these systems more energy efficient and, on top of that, to search for ways to enhance the processing speed of electronic devices.

Modern computing systems are built out of networks of transistors which use Boolean algebra. Moore's Law [1], a prediction of Gordon Moore that states that the number of transistors on a microprocessor chip would double every two years, implies that the processing speed of computing systems is improved exponentially. Hence, in order to improve the computing efficiency further, we develop faster transistors of decreasing size. However, the physical limits to the further miniaturization of the transistors, as well as the manufacturing cost, hinder the efficient growth of computing technology [2],[3]. This obstacle stimulates the quest for new trends in computing that can be used to overcome these technical and economic limitations.

A potential computing trend is neuromorphic computing. The ambition of such an endeavor is to draw inspiration from the operation of the human brain. The human brain can perform complex tasks, from processing huge amounts of unstructured data, to memorizing information and even deducing facts. The most striking difference between neuromorphic and conventional computing lies in their use of memory structures. Conventional computing relies on a basic von Neumann architecture. This architecture has several central processing units, physically separated from the main memory areas. This separation produces a temporal and energetic bottleneck, since data shuttle back and forth between the central processor and memory chips. By contrast, in both biological and artificial neural networks, the memory and the processors are collocated, meaning that they implement both memory storage as well as complex non-linear operators, used to perform distributed computation, at the same time.

Since neuromorphic computation mimics a biological brain, each part of the neuronal network must be modelled. Hence, a key challenge in building a neuromorphic computing device is to develop physical building blocks to imitate the content-based memory structures found in the brain.

Among other possible devices, memristors (from memory and resistor), have gained the spotlight as potential candidates [4],[5],[6]. Due to their dynamics, memristors can change their resistance in response to external electrical stimulation, which gives them the potential to mimic biological synapses. Moreover, memristors have desirable properties, such as non volatile memory and passivity, which make them more energy efficient than transistors. Despite the remarkable progress in the field of memristors, little is known about the dynamics of these electrical elements and their behaviour as part of a larger network of memristors, which may also include other circuit elements. As a result, expanding our understanding of the memristor is vital for the progress of the field.

1.2 Contribution

Motivated by this lack of understanding in the dynamics of memristors, we focus this thesis on investigating the possibility of using memristors as synapses for transmitting information between interconnected neurons. In order to achieve that, we consider electrical circuits with memristive elements and we study the dynamical behaviour of such circuits, and particularly the synchronization property. Neural synchronization plays a crucial role in many cognitive functions, such as memory, transferring and processing information. Initially, in this thesis we study circuits that consists of memristors and capacitors, because their simplicity allows us to focus on memristor behaviour and synchronization. Next, we replace the capacitors by FHN neurons to get a more biologically realistic model.

This thesis is structured as follows. Chapter 2 will introduce the field of memristors and present the first physical model which can be used to describe the behaviour of the memristor. In Chapter 3 , we will briefly describe some fundamental concepts of neuroscience, for instance, synapse and action potential. In addition, the dynamics of a single FHN neuron under various external stimulus is investigated.
In Chapter 4 we will introduce a mathematical framework for the modelling and analysis of dynamical systems. This mathematical framework will be utilized in Chapter 5, where electrical circuits of memristors are first coupled with capacitors, and then with FHN neurons. Here, we will also prove that these networks achieve synchronization. Finally, simulation results of capacitor -memristor networks and FHN neuron- memristor networks are drawn in Chapter 6, followed by the conclusion in the last chapter.

2 Memristor modelling

This chapter introduces the reader to the concept of memristors and memristive devices and presents an overview of some of their fundamental properties and characteristics. Then, a description of HP's memristor model is given .

2.1 The memristor

The memristor was first theorized by Dr. Leon Chua in 1971 as a new fundamental two-terminal circuit element, next to the resistor, the capacitor and the inductor [7]. In classical circuit theory there are four fundamental circuit variables, namely; the current i, the voltage v, the charge q and the flux-linkage ϕ. Chua realised that out of six possible pairwise combinations between these variables, only five had been identified. As depicted in Figure 1, the voltage is defined as the rate of change of the flux-linkage, while the current is defined as the rate of change of the charge. The remaining three relations are defined by the definition of the three fundamental passive circuit elements: the resistor, that relates the voltage and the current, the capacitor, that relates the charge and the voltage, and the inductor, that relates the flux-linkage and the current. Hence, based on simple symmetry arguments, Chua hypothesized the memristor as the missing element that relates charge and flux-linkage.

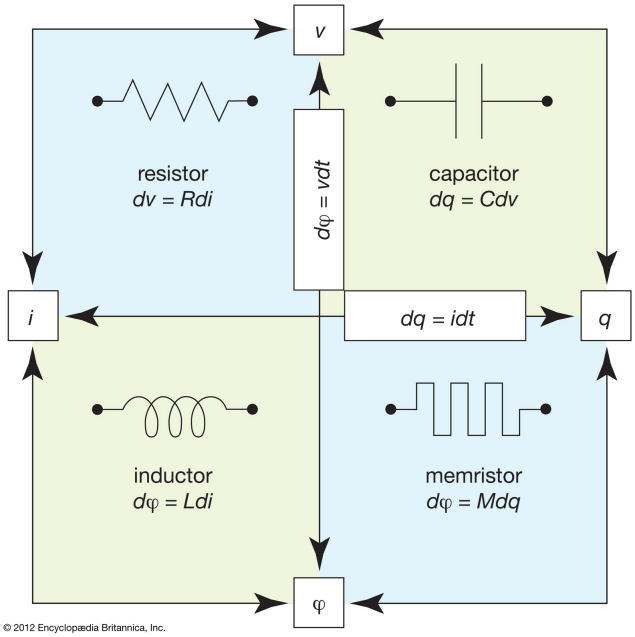

Figure 1: The four circuit variables (current i, voltage v, change q , flux-linkage ϕ) connected by the fundamental two-terminal circuit elements: resistor, capacitor, inductor, memristor, see [8].

As its name implies, the memristor, an acronym for memory and resistor, behaves as a resistor with memory, meaning that instantaneously the memristor acts as a resistor, however, its resistance changes permanently through time, depending on the resistance in the past.

A memristor is defined by a relation of the type $h(\phi(t), q(t)) = 0$. It is said to be *charge-controlled* if this relation can be expressed as a single-valued function of the charge, i.e., $\phi(t) = f(q(t))$. It is said to be *flux-controlled* if this relation can be expressed as a single-valued function of the flux-linkage as $q(t) = g(\phi(t))$.

For a charge-controlled memristor,

$$\phi(t) = f(q(t)),$$

differentiating with respect to t yields:

$$\frac{d\phi}{dt} = \frac{df(q)}{dq}\frac{dq}{dt}.$$

After substituting the voltage as $v(t) = \frac{d\phi}{dt}$ and the current as $i(t) = \frac{dq}{dt}$, the voltage across a charge-controlled memristor is given by

$$v(t) = M(q(t))i(t),$$

where

$$M(q) = \frac{df(q)}{dq}.$$

Since $M(q)$ has the unit of resistance, it will henceforth be called the *memristance*. Therefore, a charge-controlled memristor is described by

$$\begin{aligned}\dot{q}(t) &= i(t),\\ v(t) &= M(q)i(t).\end{aligned}$$

Similarly, for a flux-controlled memristor,

$$q(t) = g(\phi(t)),$$

we can obtain

$$\begin{aligned}\dot{\phi}(t) &= v(t),\\ i(t) &= W(\phi)v(t).\end{aligned}$$

Here, $W(\phi)$ has the unit of conductance, and will be referred to as *memductance*. It is defined as

$$W(\phi) = \frac{dg(\phi)}{d\phi}.$$

Observe that the memristance depends on the time integral of the current, i.e., $q(t) = \int_{-\infty}^{t} i(\tau)d\tau$ and the memductance depends on the time integral of the voltage i.e., $\phi(t) = \int_{-\infty}^{t} v(\tau)d\tau$. Thus, while the memristor instantly for $t = \tau$ behaves like an ordinary resistor, its resistance depends on the entire past history of the current and voltage. In some sense, the memristor "remembers" its previous resistance (state) and this is exactly the property that makes the memristor noteworthy.

2.1.1 Memristive device

After the introduction of the memristor, Chua and Kang [9] observed that there exist physical devices and systems whose characteristics resemble those of the memristor but cannot be realistically modelled by the definition of the memristor. Therefore, they introduced the more general notion of a memristive device given by the equations (1). Hence, the memristor is only a particular case of a general class of dynamical systems, called memristive devices and defined by

$$\begin{aligned} \dot{x}(t) &= f(x(t), u(t), t), \\ y(t) &= g(x(t), u(t), t)u(t), \end{aligned} \tag{1}$$

where $x \in \mathbb{R}^n$ denotes the state variables of the system, and the input and output signals of the system are denoted by $u(t) \in \mathbb{R}$ and $y(t) \in \mathbb{R}$, respectively. Both f and g represent continuous functions. It is assumed that system (1) has a unique solution for any initial state $x_0 \in \mathbb{R}^n$. What distinguishes the aforementioned system (1) from an arbitrary dynamical system is that the output is zero whenever the input is zero, regardless of the state x, which incorporates the memory effect.

The definition of a memristive device opens the possibility for two different types of time-invariant memristive system: the charge-controlled and the flux-controlled memristive device. An nth-order charge-controlled time-invariant memristive device is represented by

$$\begin{aligned} \dot{x} &= f(x, i), \\ v &= R(x, i)i, \end{aligned}$$

and a flux-controlled time-invariant memristive device is represented by

$$\dot{x} = f(x, v),$$
$$i = G(x, v)v,$$

where $x \in \mathbb{R}^n$ is the n-dimensional state variable of the system, $i(t)$ denotes the current through, and $v(t)$ represents the voltage across the device. As before, f is a continuous function that determines how the internal state variables evolve. The functions M and G are continuous and represent the memristance and memductance of the devices, respectively.

2.2 General properties

Memristive devices have many attractive properties, which distinguish them from the wide range of dynamical systems. Some of the most interesting properties are discussed in this section. For more details as well as for the proofs of the properties we refer the reader to [7], [9].

- **Pinched Hysteresis Loop**
  A strictly passive memristor under a sinusoidal excitation centered at zero always gives rise to a Lissajous-like hysteretic $i - v$ response crossing the origin which is at most a double-valued function of the input.

  As depicted in Figure 2 a typical response of a memristor under a sinusoidal input in an i, v diagram is a pinched hysteresis loop. This hysteresis loop crosses the origin, which implies that the output of the system equals zero whenever the input is equal to zero. Moreover, Figure 2 illustrates that the area of the hysteresis loop of a memristor decreases with the frequency of the input signal, and converges to a straight line as the frequency tends to infinity.

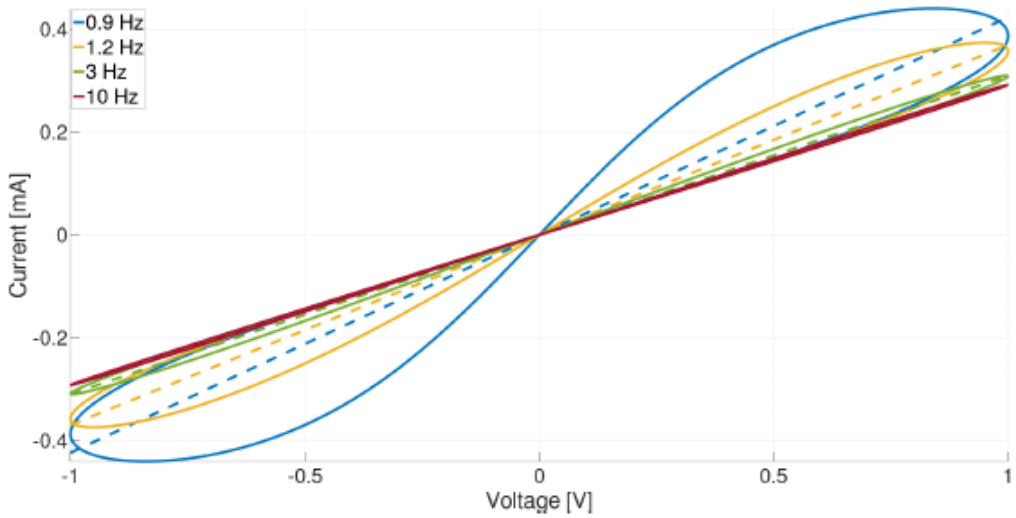

Figure 2: Pinched hysteresis loop of a memristor. The input voltage is $V(t) = \sin(2\pi f t)$ where f denotes the frequency and takes several values. The dashed lines represent the loop slope, which decreases with increasing frequency, see [10].

In addition, we assume that system (1), has a unique periodic solution $x(t)$ for all $t \geq t_0$ with the same period as that of the input signal. Hence, consider a flux-controlled memristive device, under periodic current input i with amplitude I, i.e., $i(t) \in [-I, I]$. Since the input crosses each value twice during one period, every value of i corresponds to at most two distinct values of $v(i)$. Figure 3 illustrates this property: the left figure corresponds to a memristor, because any value of i corresponds to at most two values of v, while the right figure cannot correspond to a memristor, since there is a value of i that corresponds to more than two values of v.

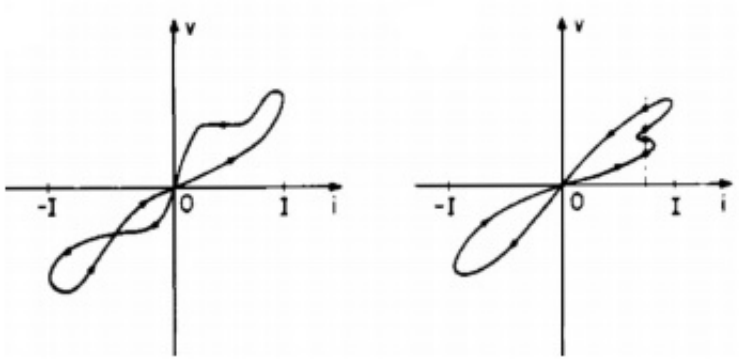

Figure 3: Left: Possible hysteresis loop. Right: Impossible hysteresis loop [9].

- **Passivity**

  A memristor characterised by a piecewise differentiable $q-\phi$ curve is passive if, and only if, its memristance is nonnegative i.e., $M(q) \geq 0$ (or memductance $W(\phi) \geq 0$) at any instant of time.

  The passivity criterion establishes that the memristor may exist in a purely passive form without the need of an internal power source to operate. This, among other properties, makes memristors potential building blocks for neuromorphic computing, since passive components are more energy-efficient than devices with internal power supply.

- **Non-volatile memory**

  Another desirable property of the memristor is that they act as non-volatile memory. Specifically, if we remove the input after a certain amount of time, and come back to use it, the device will continue its operation from the same resistance as (at least for an ideal memristor as $\dot{\phi}$ or $\dot{q}$ is zero when no input is applied) to the one in which we left it.

- **Polarity**

  Memristors react to the direction of the current, meaning that they have polarity. This property is shown on the proposed symbol of the memristor used in electronic diagrams which is depicted in Figure 4. We can observe that the symbol is not symmetric, so we can distinguish between the positive (left) and negative (right) side of the memristor.

Figure 4: Symbol of a memristor.

2.3 Physical memristor: HP model.

Despite the fact that the memristor was proposed in the early 70's, for several decades it was considered nothing more than a mathematical curiosity. It was until very recently, in 2008 when the first nanoscale solid-state device, recognised as a memristor, was fabricated by Hewlett-Packard (HP) Labs and the field of memristors was revived again [11]. More precisely, as illustrated in Figure 5, the actual device is made of a thin titanium dioxide semiconductor film of thickness D which is located between two platinum electrodes. The dioxide film can be represented by two regions, one having low resistance R_{ON}, called doped and one having high resistance R_{OFF}, called undoped. The state variable w is the absolute extent of the doped region.

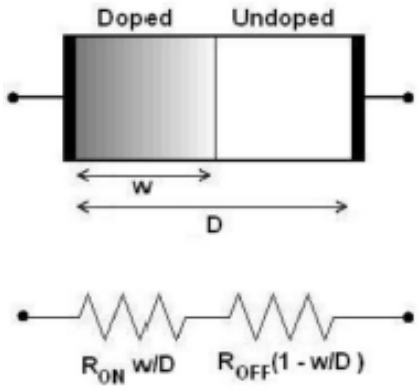

Figure 5: A graphical illustration of HP's memristor device. The semiconductor film of thickness D, has a doped and an undoped region. The resistance of each region is modelled by a variable resistor: $R_{ON}\frac{w}{D}$ for the doped and $R_{OFF}\frac{(1-w)}{D}$ for the undoped region. [11]

When an input current is applied through the memristive device, the wall separating the two regions is moving, i.e., the variable w changes. This causes the total memristance of the device to change. Thus, the total memristance of the device is modelled by two variable resistors in series, whose ratio depends on the position of the wall, as shown in Figure 5, and is described by

$$M(w(t)) = R_{ON}\frac{w(t)}{D} + R_{OFF}\left(1 - \frac{w(t)}{D}\right), \tag{2}$$

where we assume that $0 \leq w(t) \leq D$ in order that $M(w(t)) > 0$. Moreover, R_{ON} is the resistance of the the maximum conducting state and R_{OFF} represents the opposite case ($R_{ON} < R_{OFF}$). In addition, the dynamics of the memristive device can be modelled through the time dependence of the width w of the doped region. Hence, the state equation is given by

$$\frac{dw(t)}{dt} = \mu_v \frac{R_{ON}}{D} i(t). \tag{3}$$

Thus, the model is a charge-controlled memristive device given by

$$\begin{aligned} \frac{dw(t)}{dt} &= \mu_v \frac{R_{ON}}{D} i(t), \\ v(t) &= \left(R_{ON}\frac{w(t)}{D} + R_{OFF}\left(1 - \frac{w(t)}{D}\right)\right) i(t), \end{aligned}$$

where $w(t)$ is a state variable, $i(t)$ is the current through the device and $v(t)$ is the voltage drop across it.

The above system can be expressed as a function of $q(t)$ by integrating (3) in order to obtain $q(t)$,

$$w(t) = \mu_v \frac{R_{ON}}{D} q(t) + w_0,$$

and substituting $w(t)$ into (2), which gives

$$M(q(t)) = (R_{ON} - R_{OFF}) \left(\frac{\mu_v R_{ON}}{D^2} q(t) + \frac{w_0}{D} \right) + R_{OFF}.$$

3 Neuron modelling

Among other applications of memristors, the most important one is in neuromorphic circuits. Neuromorphic circuits are circuits whose operation is meant to mimic that of the human brain. Therefore we need to understand how biological neurons function. The purpose of this chapter is to introduce, based on [12], [13], some fundamental concepts of neuroscience, in particular the idea of synapses and neural spiking. Based on these concepts, two of the main dynamic neural models are briefly discussed.

3.1 Biological neuron and synapse.

Neurons or nerve cells are specialized cells that are involved in information processing in the brain. A neuron consists of three functionally distinct parts, called dendrites, soma, and axon, see Figure 6. The dendrites are where the neuron receives information in the form of signals, from other neurons. The soma controls, depending on the strength of the information, whether it is going to send out the signal or not. If the information is strong enough, the signal travels along the axon to other neurons. We refer to the sending neuron as the pre-synaptic neuron and to the receiving neuron as the post-synaptic neuron. A typical neuron makes contacts to more than 10,000 other neurons. These contact points are called synapses. Here, the pre-synaptic neuron sends signals in the form of chemicals, which are called neurotransmitters and are regarded as electrical pulses or spikes. This phenomenon is known as an action potential. When this occurs we say that the neuron fires.

Action potentials are of great significance to the functioning of the brain, since they transmit information in the nervous system. Consequently, it is of paramount importance to understand how they are propagated. Similarly to any other cell, neurons are surrounded by a cell membrane and there exist many channels allowing positive or negative ions to flow into and out of the cell. The difference in voltage between the inside and outside of the cell membrane is called membrane potential.

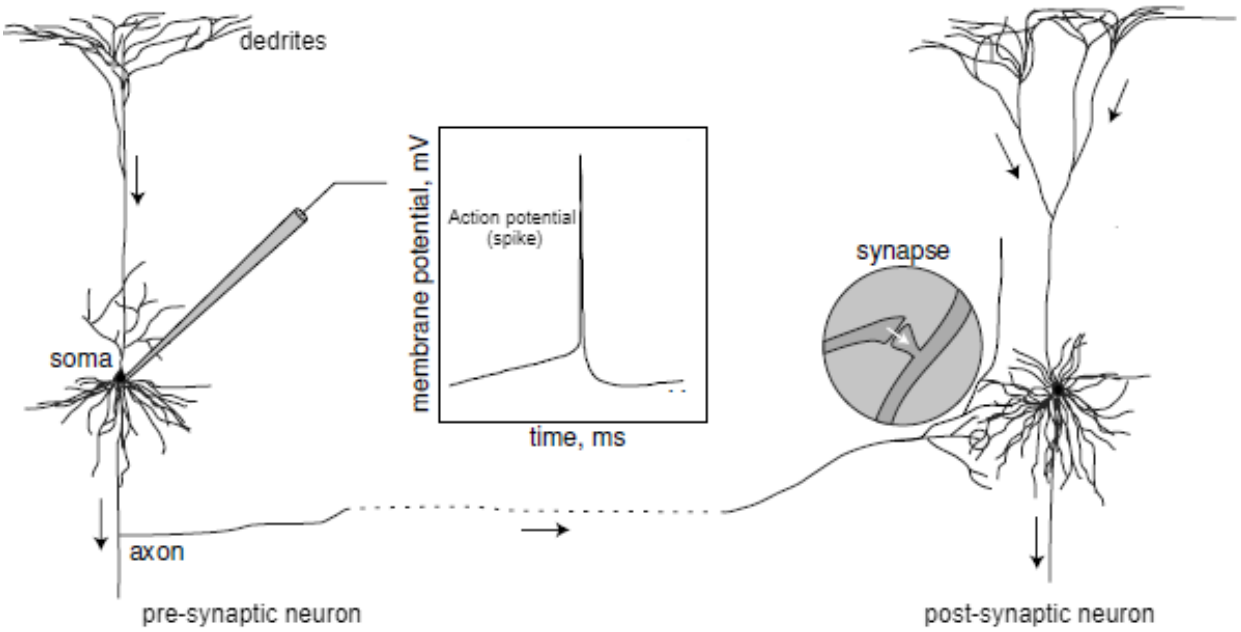

Figure 6: Schematic illustration of biological neurons and the signal transmission from a pre-synaptic neuron to a post-synaptic neuron through a synapse. The axons at the lower end lead to other neurons. The inset shows an example of a neuronal action potential. This short voltage spike will propagate along the axon of the pre-synamptic neuron to the synapses of other neurons, see [12].

A single neuron can receive thousands of synaptic inputs from many different pre-synaptic neurons. These inputs produce electrical transmembrane currents that influence the membrane potential of the neuron. Without any input, the neuron is at rest, which corresponds to a constant membrane potential. If the input increases the voltage potential we call the synapse excitatory. If the input decreases the voltage potential the synapse is called inhibitory. The type of the synapse does not change through time, however each synapse can have varying strength, called synapse weight, which depends on the ionic flow through the neurons. When the total sum of the inputs makes the neuron's membrane potential reach a certain threshold, then an action potential is generated and the membrane potential returns to the resting state. Then, the neuron is able to fire again, see Figure 7.

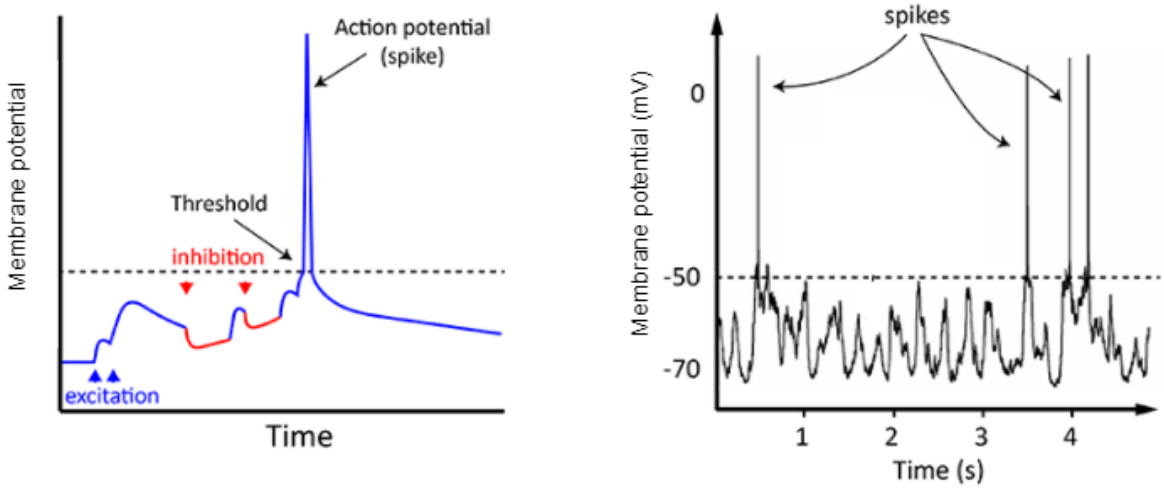

Figure 7: Left: Schematic diagram of the propagation of an action potential. A neuron fires when the total sum of the excitatory and the inhibitory synapses with the surrounding pre-synaptic neurons exceed a certain threshold. Right: Action potentials of an actual neuron in the mouse's cortex. At rest the membrane potential is about -70mV, as soon as the membrane potential reaches a certain threshold, around -50mV, its trajectory shows a spike-like excursion with an amplitude of about 100 mV. Afterwards the voltage potential returns to the rest ready to fire again.[14]

3.2 Neuron models

In this section we briefly present two of the most well-known dynamical models in computational neuroscience for capturing neural firing behaviours. First, the groundbreaking Hodgkin-Huxley model is reviewed and subsequently a simplified version, the FitzHugh-Nagumo model, is discussed.

3.2.1 Hodgkin-Huxley model (HH)

In the early 1950s, Alan Hodgkin and Andrew Huxley [15] developed a detailed mathematical model explaining how action potentials are generated along a squid giant axon. The two researchers described the dynamics of the membrane of the axon using an equivalent electrical circuit, analogous to Figure 8.

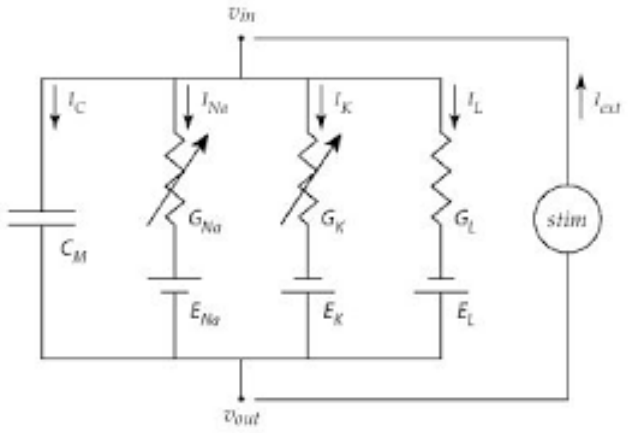

Figure 8: Electrical equivalent circuit for the dynamics of the voltage potential in the HH model, see [16].

Firstly, the membrane potential V_m is defined as $V_m = v_{in} - v_{out}$ where v_{in} and v_{out} are the potentials inside and outside the cell, respectively. Furthermore, the total current $I(t)$ across the membrane has two components, one corresponding to membrane capacitance and one corresponding to the flow of individual ions through the membrane. The capacitive current is equal to $I_C = C_m \frac{dV_m}{dt}$. The ionic current, I_{ion}, is the algebraic sum of the sodium current I_{Na}, potassium current I_K and the Ohmic leak current I_L. Based on Ohm's law, the ionic current is given by

$$I_{ion} = I_{Na} + I_K + I_L = G_{Na}(V_m - E_{Na}) + G_K(V_m - E_K) + G_L(V_m - E_L),$$

where G_{Na}, G_K, G_L represent the conductance for each ion through the membrane and E_{Na}, E_K, E_L are the equilibrium potentials for each ion i.e. the membrane potential at which there is no net movement of that ion across the membrane. Both G_{Na} and G_K are time and voltage dependent functions, while $E_{Na}, E_K, E_L, C_m, G_L$ are constants that are determined via experimentation.

Using Kirchoff's current law, the algebraic sum of all the currents entering and leaving a junction must be equal to zero, so we have $I(t) = 0$. Hence, the dynamics of the membrane can be described by

$$\begin{aligned} C_m \frac{dV}{dt} &= -\left[I_K + I_{Na} + I_L\right] + I_{ext} \\ &= -\left[G_K(V - E_K) + G_{Na}(V - E_{Na}) + G_L(V - E_L)\right] + I_{ext} \end{aligned} \tag{4}$$

where I_{ext} is an externally applied current.

If there is no stimulus applied, so $I_{ext} = 0$, the neuron remains at rest i.e. $\frac{dV}{dt} = 0$ and therefore

action potentials are not generated. If $I_{ext} \neq 0$ depending on the different types of input, we obtain different scenarios on the dynamics of the neuron.

Based on pioneering experimental techniques, Hodgkin and Huxley proposed to model the time and voltage dependence of the sodium and potassium conductance of the membrane as

$$\begin{aligned} G_{Na}(t,V) &= \bar{g}_{Na} m^3 h, \\ G_K(t,V) &= \bar{g}_K n^4, \end{aligned} \tag{5}$$

where the variables n, m, h are described through the differential equations

$$\begin{aligned} \dot{n} &= \alpha_n(V)(1-n) - \beta_n(V)n, \\ \dot{m} &= \alpha_m(V)(1-m) - \beta_m(V)m, \\ \dot{h} &= \alpha_h(V)(1-h) - \beta_h(V)h. \end{aligned}$$

The parameters $\bar{g}_{Na}, \bar{g}_K$ are called maximal conductance and describe the total number of sodium or potassium channels within the cell. The n, m, h are called gating variables and vary from 0 to 1. The variables m, h control the activation and inactivation gates of sodium channels respectively, whereas the activation gates of potassium channels are controlled by n. The functions $\alpha(V)$ and $\beta(V)$ describe the transition rates between open and closed states of the channels and they are given by

$$\begin{aligned} \alpha_n(V) &= 0.01 \frac{10-V}{\exp\left(\frac{10-V}{10}\right)-1}, \quad \beta_n(V) = 0.125 \exp\left(\frac{-V}{80}\right), \\ \alpha_m(V) &= 0.1 \frac{25-V}{\exp\left(\frac{25-V}{10}\right)-1}, \quad \beta_n(V) = 4 \exp\left(\frac{-V}{80}\right), \\ \alpha_h(V) &= 0.07 \exp\left(\frac{-V}{20}\right), \qquad \beta_n(V) = \frac{1}{\exp\left(\frac{30-V}{10}\right)+1}. \end{aligned}$$

Substituting the potassium and sodium conductance (5) in equation (4) we obtain the complete set of the Hodgkin-Huxley equations

$$\begin{aligned} C_m \frac{dV}{dt} &= -\bar{g}_K n^4 (V - E_K) - \bar{g}_{Na} m^3 h (V - E_{Na}) + \bar{g_L}(V - E_L), \\ \dot{n} &= \alpha_n(V)(1-n) - \beta_n(V)n, \\ \dot{m} &= \alpha_m(V)(1-m) - \beta_m(V)m, \\ \dot{h} &= \alpha_h(V)(1-h) - \beta_h(V)h. \end{aligned} \tag{6}$$

3.2.2 FitzHugh-Nagumo model (FHN)

A two-dimensional simplification of the Hodgkin-Huxley model was derived by FitzHugh (1961) [17] and, independently, by Nagumo et al. (1962) [18]. The FHN model is often used to describe the behaviour of a neuron and its ability to propagate an action potential. Its justification is based on the observation that the membrane voltage V and the activation of sodium current m evolve on a similar time scale, whereas the activation of potassium current n and the inactivation of sodium current h change in much slower time scales. Given these similarities, we combine V and m under a single 'voltage-like' variable V, and we couple n with $(1-h)$ into a single 'recovery' variable W.

The two equations in the FHN neuron model are then given as

$$\begin{aligned} \dot{V} &= V - \frac{V^3}{3} - W + I_{ext}, \\ \dot{W} &= c(V + a - bW). \end{aligned} \tag{7}$$

The parameters a, b and c are dimensionless and positive. The I_{ext} corresponds to an externally applied current, while the parameter c determines how fast W changes relative to V.

In order to get some insights into the dynamics of the FHN model, and how the external current influences the firing behaviour of the neuron, we analyze the nullclines of the system. In the (V, W) plane, the V-nullcline is the cubic curve $W = V - \frac{V^3}{3} + I_{ext}$ and the W-nullcline is the straight line $W = (V + a)/b$,as shown in Figure 9. Using realistic parameter values results in one point of intersection between the nullclines. Thus, the unique fixed point (V^*, W^*) of the FHN model is the solution of the system

$$\begin{aligned} V - \frac{V^3}{3} - W + I_{ext} &= 0, \\ V + a - bW &= 0. \end{aligned} \tag{8}$$

We analyze the stability of the equilibrium point by linearizing the system around it.

Let $f(V, W) = V - \frac{V^3}{3} - W + I_{ext}$ and $g(V, W) = c(V + a - bW)$. We take a point $V = V^* + x$. By differentiating it we obtain $\dot{V} = \dot{x}$. Likewise, we choose $W = W^* + y$ and we get $\dot{W} = \dot{y}$.

Taking the Taylor expansion of $\dot{V}$ and $\dot{W}$ we can write

$$\dot{x} = \frac{\partial f(V,W)}{\partial V}(V - V^*) + \frac{\partial f(V,W)}{\partial W}(W - W^*) + \textit{ high order terms,}$$
$$\dot{y} = \frac{\partial g(V,W)}{\partial V}(V - V^*) + \frac{\partial g(V,W)}{\partial W}(W - W^*) + \textit{ high order terms.}$$

Taking both x and y to be sufficiently small, we can neglect the higher order terms. Therefore, we have

$$\begin{aligned} \dot{x} &= (1 - {V^*}^2)x - y, \\ \dot{y} &= cx - cby. \end{aligned} \tag{9}$$

Expressing the system (9) as a matrix equation gives

$$\begin{pmatrix} \dot{x} \\ \dot{y} \end{pmatrix} = \begin{pmatrix} (1 - V^{*2}) & -1 \\ c & -cb \end{pmatrix} \begin{pmatrix} x \\ y \end{pmatrix}.$$

This is the Jacobian matrix and easily we compute the eigenvalues

$$\lambda_{1,2} = \frac{-V^{*2} + 1 - bc \pm \sqrt{(V^{*2} - 1 - bc)^2 - 4c}}{2}.$$

Thus, the stability of the equilibria depends on the position of the fixed point in the phase space. The solution is stable if and only if both the eigenvalues have negative real part. This happens when

$$-\sqrt{1 - bc} < V^* < \sqrt{1 - bc}.$$

Hence, we have stability whenever the W- nullcline intersects the V-nullcline along its right-and left branches.

As illustrated in Figure 9, the external stimulus I_{ext} changes the initial value of V and thereby shifts the V-nullcline. Hence, for different values of I_{ext} the fixed point can be on the left, middle, or right section of the V-nullcline.

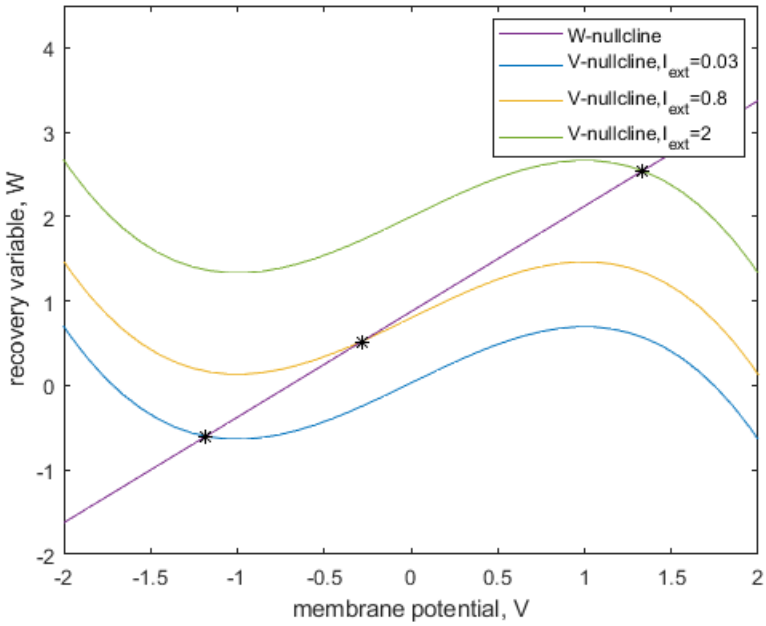

Figure 9: Nullclines of the FHN model for different values of external stimulus I_{ext} when $a = 0.7, b = 0.8, c = 0.08$.

Next, we investigate how the dynamics of the FHN model responds to different external stimulus.

When we have weak or zero stimulus, as depicted in Figure 10 the fixed point is on the left branch of V-nullcline, and the system will follow a tight trajectory around the equilibrium point and immediately return to the rest state.

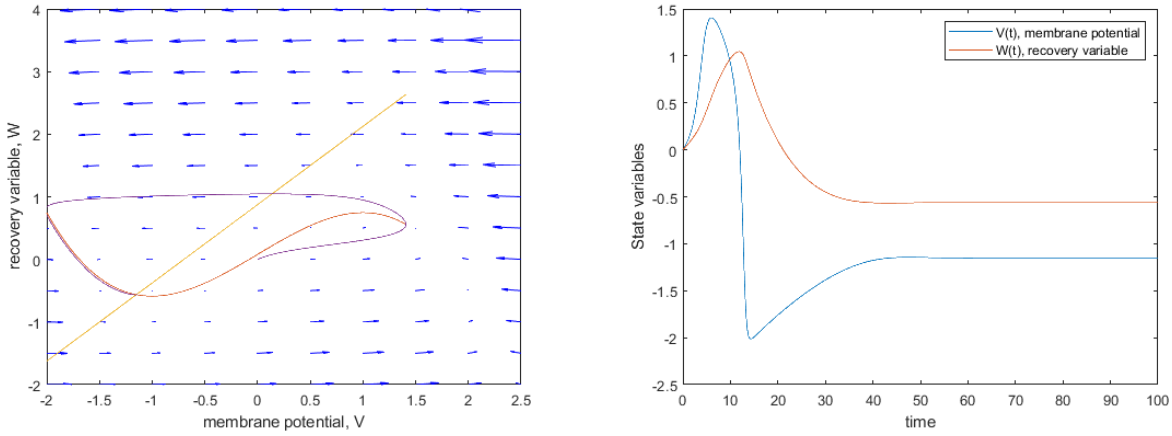

(a) Phase plane.

(b) Trajectory.

Figure 10: Phase plane and trajectory diagram of FHN model with parameters $a = 0.7, b = 0.8, c = 0.08$, and $I_{ext} = 0.08$.

As illustrated in Figure 11, by increasing the current input, the fixed point slides onto the middle branch of the V-nullcline, and becomes unstable. Because of the cubic non-linearity we observe a limit cycle oscillation in the phase plane. On the trajectory graph, infinite spiking waves can be observed, meaning that the neuron fires action potential.

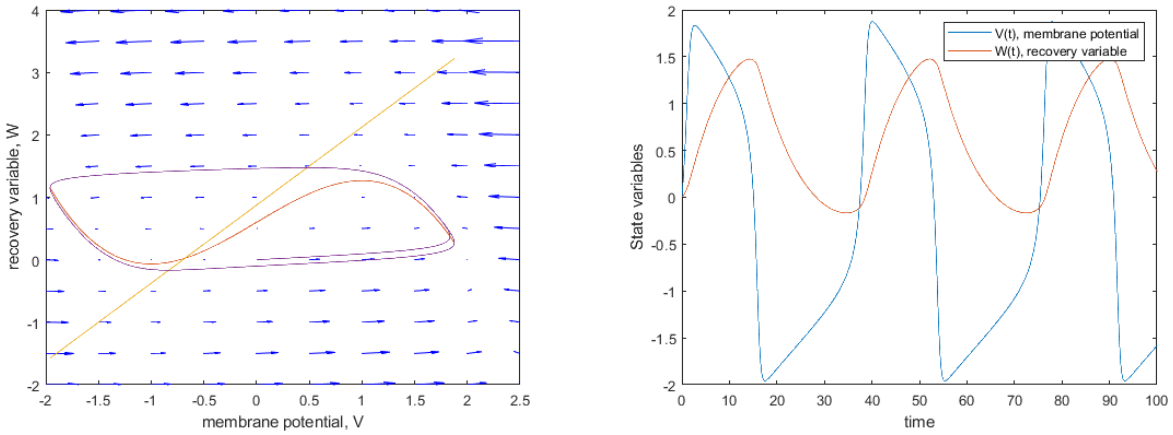

(a) Phase plane. (b) Trajectory.

Figure 11: Phase plane and trajectory diagram of FHN model with parameters $a = 0.7, b = 0.8, c = 0.08$, and $I_{ext} = 0.6$.

Increasing the external stimulus further, the fixed point is on the right section of the V-nullcline, and becomes stable, as shown in Figure 12. A fast spiking appears, which becomes damped oscillations and eventually converges to the equilibrium.

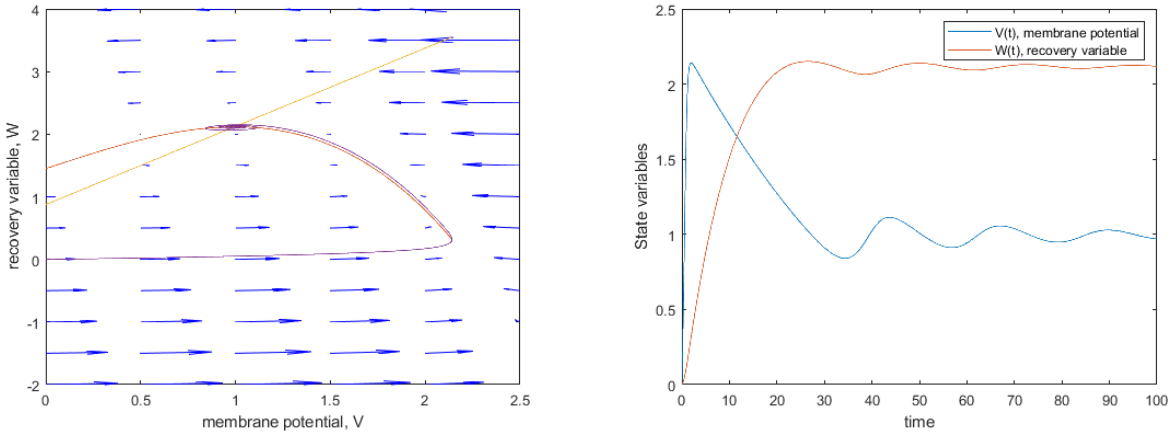

(a) Phase plane. (b) Trajectory.

Figure 12: Phase plane and trajectory diagram of FHN model with parameters $a = 0.7, b = 0.8, c = 0.08$, and $I_{ext} = 1.45$.

To summarize, despite its simplicity, the FHN model adequately reproduces the main qualitative dynamical behaviours of realistic neural models. However, the aim of the model is not to describe the physiological perspective of a neuron, but to give us an insight into the dynamical mechanism behind the firing of a neuron. We study such simpler neuron models in order to discover new phenomena, for which we can then search in more detailed biological neuron models and finally verify them through experiments.

Next, FitzHugh-Nagumo neuron model networks , in which memristors are used as an artificial synapse will be studied.

4 Mathematical framework

In this chapter we define some mathematical notions from graph theory and Lyapunov stability. These concepts will be crucial for analyzing the stability of non-linear dynamical systems in later sections.

4.1 Notation

It is helpful to start with some essential notation and terminology which will be used throughout this document.

The set of real numbers is denoted by $\mathbb{R}$, also the interval $[0, \infty)$ is denoted by $\mathbb{R}_{\geq 0}$. Let $\mathbb{R}^n$ denote the real coordinate space of dimension n and let $\mathbb{R}^n_{\geq 0}$ the subset of those real numbers that are non-negative. We denote the n-dimensional vector whose elements are 1 as $\mathbb{1}_n$, and whose elements are 0 as $\mathbb{0}_n$. The transpose of $x \in \mathbb{R}^n$ is denoted by x^T. Let vectors $x, y \in \mathbb{R}^n$, then the relationship $x \leq y$ is defined by $x_i \leq y_i$ for $i \in \{1, \ldots, n\}$, where x_i denotes the i_{th} element of x. The relations $\geq, <, >$ are defined similarly. As $||\cdot||$ we define the Euclidean norm $||x||^2 = x_1^2 + \cdots + x_n^2$ for any vector $x \in \mathbb{R}^n$, and the distance between x and y is defined by d$(x, y) = ||x - y||$. The spectrum of a matrix M is the set of its eigenvalues and is denoted as $\sigma(M)$. Moreover, the kernel of a matrix M is denoted by Ker(M) and consists of all solutions of x of the linear system $Mx = 0$.

4.2 Graph theory

This section, based on [19], [20] and [21], introduces some mathematical preliminaries from graph theory. Graph theory provides a helpful tool to model and study network systems.

Consider an undirected graph $\mathcal{G} = (\mathcal{V}, \mathcal{E})$ where $\mathcal{V} = \{v_1, v_2, \ldots, v_n\}$ is the finite set of nodes and $\mathcal{E} \subseteq \mathcal{V} \times \mathcal{V}$ the set of edges, which consists of elements of the form $\{v_i, v_j\}$ for some $i, j = 1, 2, \ldots, n$. If $\{v_i, v_j\} \in \mathcal{E}$, then the nodes v_i and v_j are said to be *adjacent*. The graph is said to be *simple* if has no self-loops or parallel edges. Moreover, the graph is said to be *connected* if there is a path joining each pair of nodes in $\mathcal{V}$. Finally, a graph is called the *complete* graph over n nodes and denoted as K_n if any node is adjacent to every other node.
Consider a simple, undirected graph $\mathcal{G} = (\mathcal{V}, \mathcal{E})$ with n nodes and m edges. Assume that an orientation has been assigned to the edges. This means that one of the nodes of a edge has the positive end and the other has the negative end.

Various matrices arise naturally in the field of graph theory. Next, we introduce the most prominent examples.

The *degree matrix* of $\mathcal{G}$, $Deg_{\mathcal{G}} \in \mathbb{R}^{n\times n}$, is the diagonal matrix whose diagonal elements are the degrees of each node, i.e. the number of edges connected to the node. The degree of the ith node is denoted by $d(v_i)$, for $i = \{1, 2, \ldots, n\}$. Hence, the degree matrix is defined as

$$Deg_{\mathcal{G}} = \begin{pmatrix} d(v_1) & 0 & \ldots & 0 \\ 0 & d(v_2) & \ldots & 0 \\ \vdots & \vdots & \ddots & \vdots \\ 0 & 0 & \ldots & d(v_n) \end{pmatrix}.$$

The *adjacency matrix* $A_{\mathcal{G}} \in \mathbb{R}^{n\times n}$ is the symmetric matrix that contains the information on the adjacency relationship in the graph $\mathcal{G}$. Its elements a_{ij} are defined as

$$a_{ij} = \begin{cases} 1, & \text{if } \{v_i, v_j\} \in \mathcal{E}, \\ 0 & \text{otherwise.} \end{cases}$$

The *incidence matrix* $D = (d_{ij}) \in \mathbb{R}^{n\times m}$ of the graph $\mathcal{G}$, is defined as

$$d_{ij} = \begin{cases} 1, & \text{if } i \text{ is the positive end of edge } j, \\ -1, & \text{if } i \text{ is the negative end of edge } j, \\ 0 & \text{otherwise.} \end{cases}$$

It can be shown that $\text{Ker}(D^T) = \text{span}\mathbb{1}_n = \{v \in \mathbb{R}^n \ : \ v = (\bar{v} \ldots \bar{v}), \bar{v} \in \mathbb{R}\}$, if the graph $\mathcal{G}$ is connected.

The *Laplacian matrix* of the graph $\mathcal{G}$, denoted by $\mathcal{L}_{\mathcal{G}}$, can be defined as $\mathcal{L}_{\mathcal{G}} = Deg_{\mathcal{G}} - A_{\mathcal{G}}$. Equivalently, it can be calculated as $\mathcal{L}_{\mathcal{G}} = DD^T$, where D is the incidence matrix of $\mathcal{G}$. In components $\mathcal{L}_{\mathcal{G}} = (l_{ij}) \in \mathbb{R}^{n\times n}$, the Laplacian matrix reads

$$l_{ij} = \begin{cases} -a_{ij}, & \text{if } i \neq j, \\ \sum_{j=1, j\neq i}^{n} a_{ij}, & \text{if } i = j. \end{cases} \tag{10}$$

where a_{ij} are the elements of the adjacency matrix $A_{\mathcal{G}}$.

A *weighted graph* $\mathcal{G} = (\mathcal{V}, \mathcal{E}, \{w_{ij}\}_{\{i,j\}\in\mathcal{E}})$ is a graph where $\{w_{ij}\}_{\{v_i,v_j\}\in\mathcal{E}}$ is a set of strictly positive numbers associated to the edges $\{v_i, v_j\} \in \mathcal{E}$ of the graph $\mathcal{G}$. The weighted Laplacian matrix $\mathcal{L}_{\mathcal{G}} = (l_{ij}) \in \mathbb{R}^{n\times n}$ of a weighted graph is defined as

$$l_{ij} = \begin{cases} -w_{ij}, & \text{if } (v_i, v_j) \in \mathcal{E}, \\ \sum_{j=1, j\neq i}^{n} w_{ij}, & \text{if } i = j, \\ 0, & \text{otherwise.} \end{cases}$$

Moreover, the weighted Laplacian can be written as

$$\mathcal{L}_{\mathcal{G}} = \mathcal{D}\mathcal{W}\mathcal{D}^T,$$

where $\mathcal{W} \in \mathbb{R}^{m\times m}$ is a diagonal matrix, with the weights $\{w_{ij}\}_{\{v_i,v_j\}\in\mathcal{E}}$ on the diagonal.
A graph $\mathcal{G} = (\mathcal{V}, \mathcal{E})$ can be regarded as a weighted graph, by setting the weights to be equal to 1 for all $\{v_i, v_j\} \in \mathcal{E}$.

We conclude this section with some useful results.

Lemma 1. *Let $\mathcal{G}$ be a simple, undirected, weighted graph on n nodes and with Laplacian $\mathcal{L}_{\mathcal{G}}$. The following properties hold:*

1. *$\mathcal{L}_{\mathcal{G}}$ is symmetric, i.e. $\mathcal{L}_G = {\mathcal{L}_{\mathcal{G}}}^T$.*
2. *$\mathcal{L}_{\mathcal{G}}$ is positive semi-definite, i.e. $x^T\mathcal{L}_{\mathcal{G}}x \geq 0$ for all $x \in \mathbb{R}^n$.*
3. *$\mathcal{L}_{\mathcal{G}}$ has n non-negative, real-valued eigenvalues: $0 = \lambda_1 \leq \lambda_2 \leq \ldots \lambda_n$. Moreover, $\lambda_2 > 0$ if and only if $\mathcal{G}$ is connected.*
4. *$\mathcal{L}_{\mathcal{G}}\mathbb{1}_n = 0_n$, i.e. 0 is an eigenvalue of $\mathcal{L}_{\mathcal{G}}$ with eigenvector $\mathbb{1}_n$.*

We refer the interested reader to [19] for the proof of the aforementioned properties.
Next, we present the Laplacian matrix and the Laplacian spectrum of the complete graph.

Lemma 2. *Let $\mathcal{G}$ be the complete graph on n nodes K_n. Then, the Laplacian of K_n is given by*

$$\mathcal{L}_{K_n} = n(I - \frac{1}{n}\mathbb{1}_n\mathbb{1}_n^T)$$

and the spectrum of $\mathcal{L}_{K_n}$, satisfies $\sigma(\mathcal{L}_{K_n}) = \{0, n, \ldots, n\}$.

Proof. From the definition of the Laplacian we have

$$\mathcal{L}_{K_n} = Deg_{K_n} - A_{K_n}. \tag{11}$$

A graph is complete if there is an edge between every pair of vertices. Therefore, each vertex of K_n has degree $(n-1)$, so

$$Deg_{K_n} = (n-1)I. \tag{12}$$

Moreover, the adjacency matrix A_{K_n} takes the form of all ones with zero on the diagonal, hence,

$$A_{K_n} = \mathbb{1}_n \mathbb{1}_n^T - I. \tag{13}$$

Substituting (12) and (13) in (11) we obtain

$$\begin{aligned} \mathcal{L}_{K_n} &= Deg_{K_n} - A_{K_n} \\ &= (n-1)I - (\mathbb{1}_n \mathbb{1}_n^T - I) \\ &= n(I - \frac{1}{n}\mathbb{1}_n \mathbb{1}_n^T). \end{aligned}$$

Now, to obtain the spectrum of $\mathcal{L}_{K_n}$, we have that the spectrum of the rank one matrix $\mathbb{1}_n \mathbb{1}_n^T$ is $\{0, 0, \ldots, 0, n\}$. Moreover, we observe that the addition of the matrix nI shifts all eigenvalues of matrix $\mathbb{1}_n \mathbb{1}_n^T$ by n. Hence,

$$\sigma(\mathcal{L}_{K_n}) = \{0, n, \ldots, n\}.$$

□

Based on the definition of the Laplacian matrix we provide a useful equality.

Lemma 3. *Let $\mathcal{G} = (\mathcal{V}, \mathcal{E})$ be a simple undirected graph on n nides and with Laplacian matrix $\mathcal{L}_{\mathcal{G}}$. For any $x, y \in \mathbb{R}^n$,*

$$y^T \mathcal{L}_{\mathcal{G}} x = \sum_{\{v_i, v_j\} \in \mathcal{E}}^{n} a_{ij}(y_i - y_j)(x_i - x_j).$$

Proof. First, for all rows i of the Laplacian and for any $x \in \mathbb{R}^n$ we have

$$(\mathcal{L}_{\mathcal{G}} x)_i = \sum_{j=1}^{n} l_{ij} x_j = l_{ii} x_i + \sum_{j=1, j \neq i}^{n} l_{ij} x_j. \tag{14}$$

After using the definition of the Laplacian (10) in (14) we obtain

$$(\mathcal{L}_{\mathcal{G}}x)_i = \sum_{j=1,j\neq i}^{n} a_{ij}x_i + \sum_{j=1,j\neq i}^{n} (-a_{ij})x_j = \sum_{j=1,j\neq i}^{n} a_{ij}(x_i - x_j).$$

Second, we compute:

$$\begin{aligned} y^T\mathcal{L}_{\mathcal{G}}x &= \sum_{i=1}^{n} y_i(\mathcal{L}_{\mathcal{G}}x)_i = \sum_{i=1}^{n} y_i\Big(\sum_{j=1,j\neq i}^{n} a_{ij}(x_i - x_j)\Big) \\ &= \sum_{i=1,j=1}^{n} a_{ij}y_i(x_i - x_j) = \sum_{i=1,j=1}^{n} a_{ij}y_ix_i - \sum_{i=1,j=1}^{n} a_{ij}y_ix_j \\ &= \frac{1}{2}\sum_{i=1,j=1}^{n} a_{ij}y_ix_i + \frac{1}{2}\sum_{i=1,j=1}^{n} a_{ij}y_ix_i - \frac{1}{2}\sum_{i=1,j=1}^{n} a_{ij}y_ix_j - \frac{1}{2}\sum_{i=1,j=1}^{n} a_{ij}y_ix_j. \end{aligned}$$

The Laplacian is symmetric therefore $a_{ij} = a_{ji}$ and we can write

$$\begin{aligned} y^T\mathcal{L}_{\mathcal{G}}x &= \frac{1}{2}\sum_{i=1,j=1}^{n} a_{ij}y_ix_i + \frac{1}{2}\sum_{i=1,j=1}^{n} a_{ij}y_jx_j - \frac{1}{2}\sum_{i=1,j=1}^{n} a_{ij}y_ix_j - \frac{1}{2}\sum_{i=1,j=1}^{n} a_{ij}y_jx_i \\ &= \frac{1}{2}\sum_{i=1,j=1}^{n} a_{ij}(y_ix_i + y_jx_j - y_ix_j - y_jx_i). \end{aligned}$$

Recall that $a_{ij} = 0$ if $\{v_i, v_j\} \notin \mathcal{E}$ therefore,

$$y^T\mathcal{L}_{\mathcal{G}}x = \sum_{\{v_i,v_j\}\in\mathcal{E}}^{n} a_{ij}(y_i - y_j)(x_i - x_j),$$

which finalizes the proof. □

Using this result, we have for the complete graph K_n, that $a_{ij} = 1$ for all $i \neq j$. In this case,

$$y^T\mathcal{L}_{K_n}x = \sum_{i=1,j=1}^{n} (y_i - y_j)(x_i - x_j).$$

Next, we introduce the Courant-Fischer Theorem , which can be useful for obtaining bounds on the eigevalues of symmetric matrices.

Theorem 4. *(Courant-Fischer).*
Let A be an $n \times n$ symmetric matrix with eigenvalues $\lambda_1 \leq \lambda_2 \leq \cdots \leq \lambda_n$ and corresponding

eigenvectors $v_1, v_2, \ldots, v_n$. *Then,*

$$\lambda_1 = \min_{||x||=1} x^T A x = \min_{x \neq 0} \frac{x^T A x}{x^T x},$$
$$\lambda_2 = \min_{||x||=1, x \perp v_1} x^T A x = \min_{x \neq 0, x \perp v_1} \frac{x^T A x}{x^T x},$$
$$\lambda_n = \max_{||x||=1} x^T A x = \max_{x \neq 0} \frac{x^T A x}{x^T x}.$$

Proof for the Courant-Fischer theorem is provided by [22] .

Let a weighted graph $\mathcal{G} = \big(\mathcal{V}, \mathcal{E}, \{g(\phi_{ij})\}_{\{v_i, v_j\} \in \mathcal{E}}\big)$, where the weight associated to every edge $\{v_i, v_j\} \in \mathcal{E}$ is determined by the function $g(\phi)$. We assume that the function $g(\phi)$ is bounded from below. Consequently, the dependent weighted Laplacian $\mathcal{L}_{\mathcal{G}}(\phi)$ of $\mathcal{G}$ is defined by $\mathcal{L}_{\mathcal{G}}(\phi) = DG(\phi)D^T$, where $G(\phi) = \text{diag}(g(\phi_{ij})_{\{v_i, v_j\} \in \mathcal{E}})$ is a diagonal positive definite matrix with $g(\phi_{ij})_{\{v_i, v_j\} \in \mathcal{E}}$ as its entries.

Lemma 5. *Consider a connected weighted graph* $G = \big(V, \mathcal{E}, \{g(\phi_{ij})\}_{\{v_i, v_j\} \in \mathcal{E}}\big)$ *with incidence matrix* $D \in \mathbb{R}^{n \times m}$. *Then the dependent weighted Laplacian* $\mathcal{L}(\phi) = DG(\phi)D^T$ *is symmetric and positive semi-definite, and for each* $\phi \in \mathbb{R}^m$ *and for any* $p \in \mathbb{R}^n$, *it holds*

$$p^T \mathcal{L}_{\mathcal{G}}(\phi) p \geq \frac{g_{min} \lambda_2(DD^T)}{n} p^T \mathcal{L}_{K_n} p$$

where g_{min} *is a lower bound on* $g(\cdot)$ *,i.e,* $g_{min} \leq g(\phi)$ *for all* $\phi \in \mathbb{R}^m$. *Moreover,* $\lambda_2(DD^T)$ *is the second smallest eigenvalue of the matrix* DD^T.

Proof. For any $p \in \mathbb{R}^n$ and $\phi \in \mathbb{R}^m$ we have

$$p^T \mathcal{L}_{\mathcal{G}}(\phi) p = p^T (DG(\phi)D^T) p = \sum_{\{v_i, v_j\} \in \mathcal{E}}^{n} g(\phi_i)(p_i - p_j)^2 \geq 0, \tag{15}$$

as follows in a similar way as the result of Lemma 3. Hence, the dependent weighted Laplacian is positive semi-definite.

Let g_{min} a lower bound of $g(\phi)$, it follows from equality (15) that

$$p^T (DG(\phi)D^T) p \geq g_{min} \sum_{i,j \in \mathcal{E}}^{n} (p_i - p_j)^2 = g_{min} p^T DD^T p. \tag{16}$$

Since the inequality (16) holds for any vector $p \in \mathbb{R}^n$ take $p = c\mathbb{1} + v$ where $c \in \mathbb{R}$ and the vector v is orthogonal to $\mathbb{1}$. Thus, the inequality becomes

$$p^T \mathcal{L}_{\mathcal{G}}(\phi) p \geq g_{min}(c\mathbb{1} + v)^T DD^T (c\mathbb{1} + v) = g_{min} v^T DD^T v. \tag{17}$$

The last equality holds, since the graph $\mathcal{G}$ is connected i.e. $D^T \mathbb{1} = 0$.
Now, applying the theorem Courant-Fischer (Theorem 4) for the Laplacian matrix DD^T we get

$$\lambda_2(DD^T) = \min_{v \neq 0, v \perp \mathbb{1}} \frac{v^T DD^T v}{v^T v},$$

such that

$$v^T DD^T v \geq \lambda_2(DD^T) v^T v,$$

for all $v \perp \mathbb{1}$.
Substituting this result into (17) we obtain a lower bound for the dependent weighted Laplacian as

$$p^T \mathcal{L}_{\mathcal{G}}(\phi) p \geq g_{min} \lambda_2(DD^T) v^T v. \tag{18}$$

Likewise, for the Laplacian of a complete graph $\mathcal{L}_{K_n}$ by choosing $p = c\mathbb{1} + v$ we get

$$p^T \mathcal{L}_{K_n} p = (c\mathbb{1} + v)^T \mathcal{L}_{K_n} (c\mathbb{1} + v) = v^T \mathcal{L}_{K_n} v \leq \lambda_n(\mathcal{L}_{K_n}) v^T v.$$

By Lemma 2, it follows that the largest eigenvalue of $\mathcal{L}_{K_n}$ is $\lambda_n(\mathcal{L}_{K_n}) = n$, therefore an upper bound for $\mathcal{L}_{K_n}$ is

$$p^T \mathcal{L}_{K_n} p \leq n v^T v. \tag{19}$$

Finally, (18) can be rewritten as

$$p^T \mathcal{L}_{\mathcal{G}}(\phi) p \geq \frac{g_{min} \lambda_2(DD^T)}{n} n v^T v,$$

after which substituting from inequality (19) leads to

$$p^T \mathcal{L}_{\mathcal{G}}(\phi) p \geq \frac{g_{min} \lambda_2(DD^T)}{n} p^T \mathcal{L}_{K_n} p$$

for any $p \in \mathbb{R}^n$, $\phi \in \mathbb{R}^m$. □

4.3 Lyapunov stability

In this section, based on [23],[24], we review basic concepts from Lyapunov stability theory with emphasis on global asymptotic stability with respect to sets. We start with some basic definitions.

Consider the dynamical system

$$\dot{x} = f(x(t), u(t), t)$$
$$y = h(x(t), u(t), t),$$

where $x(t) \in \mathbb{R}^n$ is the state vector, $u(t) \in \mathbb{R}^m$ is referred to as input vector and $y(t) \in \mathbb{R}^p$ as output vector. The smooth maps $f : \mathbb{R}^n \times \mathbb{R}^m \to \mathbb{R}^n$ and $h : \mathbb{R}^n \to \mathbb{R}^p$ describe the dynamics for the system. If f and h do not explicitly depend on time t, then the system is called *time-invariant*, otherwise it is called *time-varying*. A system is *forward complete* if for every initial condition the corresponding solution is defined for all $t \geq 0$. In case there are no input variables u, and the system is time-invariant, the system takes the form

$$\dot{x} = f(x(t)). \tag{20}$$

The function f is assumed to satisfy the following conditions for the existence and uniqueness of solutions. First, f is continuous in x. Moreover,it is locally Lipschitz in x, that is, for each compact set $K \subset \mathbb{R}^n$ there exists some constant L such that $||f(x) - f(y)|| \leq L||x - y||$ for all $x, y \in K$. We denote by $x(t, x_0)$ the solution at time t of system (20) with initial condition $x(0) = x_0$.

Some comparison functions are next defined. These are used in many statements in non-linear control theory. For more details on such comparison functions see [25].

Definition 6. *A continuous function $\alpha : \mathbb{R}_{\geq 0} \to \mathbb{R}_{\geq 0}$ is said to be a $\mathcal{K}$-function if is strictly increasing and $\alpha(0) = 0$. It is said to be a $\mathcal{K}_\infty$ function if, in addition $\alpha(s) \to \infty$ as $s \to \infty$.*

Definition 7. *A continuous function $\beta : R_{\geq 0} \times \mathbb{R}_{\geq 0} \to \mathbb{R}_{\geq 0}$ is said to $\mathcal{KL}$-function if, for each fixed s, the mapping $\beta(r, s)$ is a $\mathcal{K}$-function with respect to r and, for each fixed r, the mapping $\beta(r, s)$ is decreasing with respect to s and $\beta(r, s) \to 0$ as $s \to \infty$.*

We call a state $x^* \in \mathbb{R}^n$ an *equilibrium point* of (20) if $f(x^*) = 0$. A dynamical system can have zero, one or more equilibrium points. Intuitively speaking, an equilibrium point is *stable* if trajectories which start close to it remain close to it, and *unstable* if they do not. An equilibrium point is *asymptotically stable* if it is stable and in addition the trajectories that started close enough

to x^* converge to it as as time tends to infinity.

Instead of equilibrium points, attractors can be closed subsets $\mathcal{A}$ of the state space.

Definition 8. *A set of states $\mathcal{A} \subset \mathbb{R}^n$ is called an invariant set of system (20) if for all $x_0 \in \mathcal{A}$ and for all $t \geq 0$, $x(t) \in \mathcal{A}$.*

For example, the equilibrium points of (20) are a special class of invariant sets.

Next, we introduce the following notation for the distance between a point and a set. Let $\mathcal{A} \subset \mathbb{R}^n$ be a nonempty set and $\xi \in \mathbb{R}^n$. Then, we denote the distance of ξ from $\mathcal{A}$ as

$$|\xi|_{\mathcal{A}} = d(\xi, \mathcal{A}) = \inf_{\eta \in \mathcal{A}} d(\xi, \eta).$$

For instance, the equilibrium point x^* of (20) can be represented by the set

$$\mathcal{A} = \{x \in \mathbb{R}^n \ : \ x = x^*\},$$

for which the point-to-set distance is $|x|_{\mathcal{A}} = \inf_{\eta \in \mathcal{A}} \{|x - \eta|\} = |x - x^*|$.

For stability of sets we use the definitions and theorems from [26].

Definition 9. *System (20) is globally asymptotically stale (GAS) with respect to a closed invariant set $\mathcal{A} \subset \mathbb{R}^n$ if it is forward complete and there exists a $\mathcal{KL}-$function β such that, given any initial state x_0, the solution $x(t, x_0)$ satisfies*

$$|x(t, x_0)|_{\mathcal{A}} \leq \beta(|x_0|_{\mathcal{A}}, t), \quad \forall t \geq 0.$$

When set $\mathcal{A}$ is compact, the forward completeness assumption is redundant, since in this case the solutions of the system are bounded.

In order to introduce Lyapunov functions with respect to set, the Lie derivative of a function is defined.

Definition 10. *Let $V : \mathbb{R}^n \to \mathbb{R}$ a differentiable function, and $f : \mathbb{R}^n \to \mathbb{R}^n$. Then, the Lie derivative of V with respect to f is the scalar function defined by*

$$\mathcal{L}_f V(x) = \frac{\partial V}{\partial x}(x) f(x).$$

Next, we introduce the concept of Lyapunov function which is widely used to verify if a dynamical system is asymptotically stable.

Definition 11. *A smooth Lyapunov function for the system (20) with respect to a nonempty, closed, invariant set $\mathcal{A} \subseteq \mathbb{R}^n$ is a function $V : \mathbb{R}^n \to \mathbb{R}$ such that:*

1. *there exist functions $\alpha_1, \alpha_2 \in \mathcal{K}_\infty$ such that*

$$\alpha_1(|x|_{\mathcal{A}}) \leq V(x) \leq \alpha_2(|x|_{\mathcal{A}}), \quad \forall x \in \mathbb{R}^n,$$

2. *there exists a positive definite continuous function α_3 such that*

$$\mathcal{L}_f V(x) \leq -\alpha_3(|x|_{\mathcal{A}}), \quad \forall x \in \mathbb{R}^n / \mathcal{A}.$$

Using these definitions, the following theorem from [26] allows us to determine stability for the system with respect to $\mathcal{A}$. The first theorem is for general closed, invariant sets and assumes completeness of the system.

Theorem 12. *Assume that the system (20) is forward complete. Let $\mathcal{A} \subseteq \mathbb{R}^n$ be a nonempty, closed, invariant set for this system. Then, system* (20) *is GAS with respect to $\mathcal{A}$ if and only if there exists a smooth Lyapunov function V with respect to $\mathcal{A}$.*

The following theorem is an equivalent result. However, it does not assume forward completeness, instead it applies only to compact set $\mathcal{A}$.

Theorem 13. *Let $\mathcal{A} \subseteq \mathbb{R}^n$ be a nonempty, compact, invariant set for system* (20)*. Then,* (20) *is GAS with respect to $\mathcal{A}$ if and only if there exists a smooth Lyapunov function V with respect to $\mathcal{A}$.*

5 Electrical circuits with memristors

In this chapter, with the use of graph theory, we provide a general mathematical description of networks of memristive devices coupled first with capacitors and next with FitzHugh-Nagumo neurons. We will study the dynamics of the networks and particularly the synchronization property, since synchronization is one of the fundamental issues in understanding the behaviour of chaotic -nonlinear systems.

5.1 Electrical networks

In this section we will express resistive electrical circuits in terms of graphs based on [20].

Consider a simple, undirected, connected, weighted graph $\mathcal{G} = \left(\mathcal{V}, \mathcal{E}, \{w_{ij}\}_{\{i,j\}\in\mathcal{E}}\right)$ with n nodes and m edges. Let $D \in \mathbb{R}^{n\times m}$ denote the incidence matrix that specifies the structure of the graph. We denote by $p = \begin{pmatrix} p_1 & p_2 & \dots & p_n \end{pmatrix}^T$ the vector of voltage potentials at the nodes, and by $j = \begin{pmatrix} j_1 & j_2 & \dots & j_n \end{pmatrix}^T$ the vector of nodal currents leaving the nodes. Furthermore, let $v = \begin{pmatrix} v_1 & v_2 & \dots & v_m \end{pmatrix}^T$ define the vector of voltages across the edges and $i = \begin{pmatrix} i_1 & i_2 & \dots & i_m \end{pmatrix}^T$ the vector of currents through the edges. An example of this notation is given in Figure 13.

In order to find a relation between the voltage potentials and the voltages across the edges, and between the nodal currents and the currents through the edges, we need to introduce Kirchhoff's voltage and current law e.g, [27].

Kirchhoff's voltage law.
For any electric circuit, the algebraic sum of the voltages around any closed loop is zero, at any time.

Kirchhoff's current law.
For any electric circuit, the total current entering a node is exactly equal to the charge leaving the node, at any time.

Considering the aforementioned theorems, and based on [28] we can derive a model for resistive networks. We deduce that the voltages across the edges v are equal to

$$v = \mathcal{D}^T p.$$

Similarly, the nodal currents j are equal to

$$j = -\mathcal{D}i.$$

Furthermore, in each edge of the graph has been assigned a real number $\{w_{ij}\}_{\{i,j\}\in\mathcal{E}}$ representing the conductance on this edge and let $W = \text{diag}\left(\{w_{ij}\}_{\{i,j\}\in\mathcal{E}}\right) \in \mathbb{R}^{m\times m}$. According to Ohm's law, a relationship between the voltage, the current and the conductance along the edges is given by

$$i = Wv.$$

Combining the above relations, we obtain a relation between the nodal currents and voltage potentials as

$$j = -DWD^T p,$$

where the matrix $\mathcal{L} = DWD^T$ is the weighted Laplacian of the graph.

5.2 Circuits with capacitors and memristors

In this section, building on the aforementioned result, we will describe and discuss the formation and synchronization of an electrical circuit containing capacitors and memristors.

5.2.1 Model description

Consider an electrical network of memristors and capacitors as illustrated in $Figure\ 13$. We regard this circuit as a graph in which the edges corresponds to memristors and where grounded capacitors are connected to the nodes.
Each memristor is time-invariant and the memductance g is not an explicit function of the port voltage v and it is positive for every state ϕ. The dynamics of the memristor situated at the edge k is represented by

$$\begin{aligned} \dot{\phi_k}(t) &= v_k(t), \\ i_k(t) &= g(\phi_k)v_k(t), \end{aligned} \tag{21}$$

where ϕ_k and i_k denote the flux-linkage and current at the edge k, respectively.
For the capacitor at the node s the dynamics is given by

$$c_s\dot{p_s}(t) = j_s(t), \tag{22}$$

where c_s is a positive constant that denotes the capacitance. Moreover, p_s and j_s stand for the voltage potential and current at node s, respectively.

Let $\mathcal{G} = (\mathcal{V}, \mathcal{E}, \{g(\phi_k)\}_{k\in\mathcal{E}})$ a simple undirected, connected, weighted graph with n nodes and m edges. The weights $g(\phi_k)$ describe the memductance of the memristor and depend on the dynamics (21). In addition, the orientation of the graph is given by the orientation of the memristor and is described in the incidence matrix D.
As before, we denote as $v = \begin{pmatrix} v_1 & v_2 & \dots & v_m \end{pmatrix}^T$ the vector of voltages across the edges and $i = \begin{pmatrix} i_1 & i_2 & \dots & i_m \end{pmatrix}^T$ the vector of currents through the edges. Moreover, let $p = \begin{pmatrix} p_1 & p_2 & \dots & p_n \end{pmatrix}^T$ the vector of voltage potentials at the nodes, and $j = \begin{pmatrix} j_1 & j_2 & \dots & j_n \end{pmatrix}^T$ the vector of nodal currents. In addition, we define as $\phi = \begin{pmatrix} \phi_1 & \phi_2 & \dots & \phi_m \end{pmatrix}^T$ the vector of flux-linkage through the edges.
Having these in mind, we are ready to define the dynamics of the network.

Substituting the dynamics of the memristor (21) and dynamics of capacitors (22) the dynamics of the network can be represented by

$$\begin{aligned} C\dot{p} &= -DG(\phi)D^T p, \\ \dot{\phi} &= D^T p, \end{aligned} \tag{23}$$

where $C = \text{diag}\{c_1, \dots, c_n\} \in \mathbb{R}^{n\times n}$, is a matrix having as entries the capacitance of the capacitors and $G(\phi) = \text{diag}\{g(\phi_1), \dots, g(\phi_m)\} \in \mathbb{R}^{m\times m}$ is a matrix whose elements represent the memductance of the memristors. Both matrices C and $G(\phi)$ are positive definite for each $\phi \in \mathbb{R}^m$.

We define the weighted Laplacian of the graph $\mathcal{G}$ as $\mathcal{L}(\phi) = DG(\phi)D^T$, such that the dynamics (23) can be written as

$$\begin{aligned} C\dot{p} &= -\mathcal{L}(\phi)p, \\ \dot{\phi} &= D^T p. \end{aligned} \tag{24}$$

5.2.2 Example

In this section an example of the notation and the dynamics of these networks is provided.

Consider the electrical network in Figure 13. The network consists of three memristors with mem-

ductance $g(\phi)$ and dynamics

$$\dot{\phi_k}(t) = v_k(t),$$
$$i_k(t) = g(\phi_k)v_k(t),$$

where $k \in \{1, 2, 3\}$,
and three capacitors with dynamics

$$c_s\dot{p_s}(t) = j_s(t),$$

where $s \in \{1, 2, 3\}$.

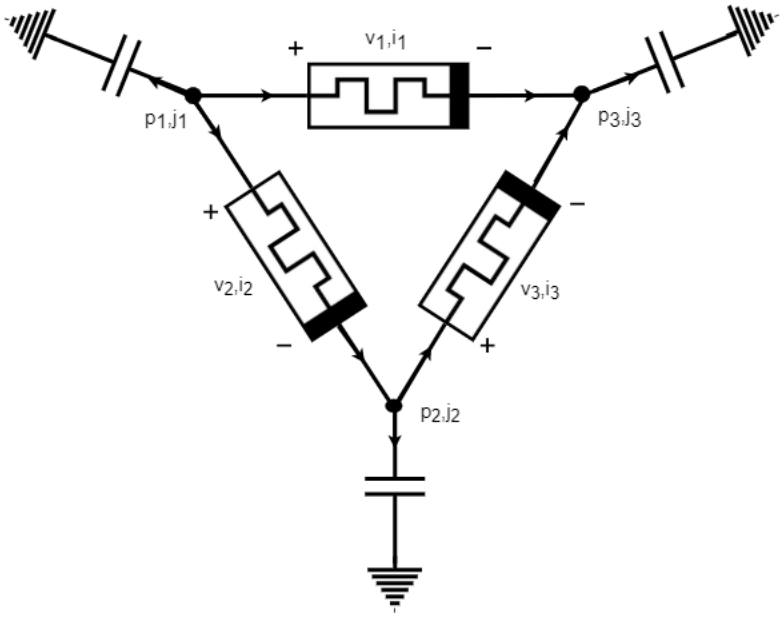

Figure 13: Network of 3 memristive devices and 3 capacitors. Here, $p = (p_1, p_2, p_3)$ and $j = (j_1, j_2, j_3)$ denote the voltage potentials and the currents and the nodes, respectively. Moreover, the voltage and current across the edges are denoted by $v = (v_1, v_2, v_3)$ and $i = (i_1, i_2, i_3)$, respectively.

The incidence matrix D of the graph, and the matrices $G(\phi)$ and C are given by

$$D = \begin{pmatrix} 1 & 1 & 0 \\ 0 & -1 & 1 \\ -1 & 0 & -1 \end{pmatrix}, \quad G(\phi) = \begin{pmatrix} g(\phi_1) & 0 & 0 \\ 0 & g(\phi_2) & 0 \\ 0 & 0 & g(\phi_3) \end{pmatrix}, \quad C = \begin{pmatrix} c_1 & 0 & 0 \\ 0 & c_2 & 0 \\ 0 & 0 & c_3 \end{pmatrix}.$$

As result, according to (24), the dynamics of the network is described by

$$\begin{aligned}
c_1\dot{p_1} &= g(\phi_1)(p_3 - p_1) + g(\phi_2)(p_2 - p_1),\\
c_2\dot{p_2} &= g(\phi_2)(p_1 - p_2) + g(\phi_3)(p_3 - p_2),\\
c_3\dot{p_3} &= g(\phi_1)(p_1 - p_3) + g(\phi_3)(p_2 - p_3),\\
\dot{\phi_1} &= p_1 - p_3,\\
\dot{\phi_2} &= p_1 - p_2,\\
\dot{\phi_3} &= p_2 - p_3.
\end{aligned}$$

5.2.3 Proof of synchronization

In this section, the objective is to prove that the memristor - capacitor network is synchronized. The concept of synchronization refers to making identical chaotic dynamical systems with different initial conditions oscillate in a synchronized manner. We will show synchronization, by proving that the network is globally asymptotically stable (GAS) with respect to a closed invariant set $\mathcal{A}$.

Consider a network of n capacitors and m memristors. Recall that the dynamics of this network can be described by

$$\begin{aligned}
C\dot{p} &= -\mathcal{L}(\phi)p,\\
\dot{\phi} &= D^T p.
\end{aligned} \tag{25}$$

Let $x = \begin{pmatrix} Cp & \phi \end{pmatrix}^T \in \mathbb{R}^{n+m}$ be the state vector, then the system is of the form

$$\dot{x} = f(x),$$

where $f(x)$ is given by

$$f(x) = \begin{pmatrix} -\mathcal{L}(\phi)p \\ D^T p \end{pmatrix},$$

which is a time-invariant and forward complete system. Using definitions and theorems from Section 4.3 we can show that the system is GAS.

First we determine the equilibrium points of the system (25) by solving the equation $f(x) = 0$.

This leads to

$$\left.\begin{matrix} -\mathcal{L}(\phi)p = 0 \\ D^T p = 0 \end{matrix}\right\} \implies \begin{matrix} p = b\mathbb{1}_n,\ b \in \mathbb{R}, \\ \phi \in \mathbb{R}^m. \end{matrix}$$

We represent the equilibrium points of (25) by the set

$$\mathcal{A} = \left\{ x = \begin{pmatrix} Cp \\ \phi \end{pmatrix} \in \mathbb{R}^{n+m} : p = b\mathbb{1}_n, b \in \mathbb{R}, \phi \in \mathbb{R}^m \right\}.$$

The set $\mathcal{A}$ is invariant since it consists of all the equilibrium points of the system (25).

Next we define the distance from a point $x \in \mathbb{R}^{n+m}$ to the set $\mathcal{A}$.

Lemma 14. *Consider the vector* $x = \begin{pmatrix} Cp & \phi \end{pmatrix}^T \in \mathbb{R}^{n+m}$. *Let* $\mathcal{A} \subset \mathbb{R}^{n+m}$, *with* $\mathcal{A} = \{x \in \mathbb{R}^{n+m} : p = b\mathbb{1}_n, b \in \mathbb{R}, \phi \in \mathbb{R}^m\}$ *be a nonempty, closed, compact, invariant set. Then the distance between a point* $x \in \mathbb{R}^{n+m}$ *and the set* $\mathcal{A}$, *denoted by* $|x|_{\mathcal{A}}$, *is given by*

$$|x|_{\mathcal{A}}^2 = \left| (I - \frac{1}{N}\mathbb{1}_n\mathbb{1}_n^T)Cp \right|^2.$$

Proof. Let $x = \begin{pmatrix} Cp & \phi \end{pmatrix}^T \in \mathbb{R}^{n+m}$. The distance between x and a set is the infimum of the distances between the point and those in the set, hence

$$|x|_{\mathcal{A}}^2 = d(x, \mathcal{A})^2 = \inf_{\eta \in \mathcal{A}} d(x, \eta)^2 = \inf_{\eta \in \mathcal{A}} \left| \begin{pmatrix} Cp \\ \phi \end{pmatrix} - \eta \right|^2, \tag{26}$$

using the definition of the set $\mathcal{A}$, (26) is equivalent to

$$|x|_{\mathcal{A}}^2 = \inf_{b \in \mathbb{R}} \left| \begin{pmatrix} Cp \\ \phi \end{pmatrix} - \begin{pmatrix} b\mathbb{1}_n \\ \phi \end{pmatrix} \right|^2 = \inf_{b \in \mathbb{R}} |Cp - b\mathbb{1}_n|^2. \tag{27}$$

In order to determine the $b \in \mathbb{R}$ that minimizes the above distance we take the least square approach. Multiplying by $\mathbb{1}_n^T$ leads to

$$b^*\mathbb{1}_n^T\mathbb{1}_n = \mathbb{1}_n^T Cp \implies b^* = \frac{1}{n}\mathbb{1}_n^T Cp.$$

Thus, for $b^* = \frac{1}{n}\mathbb{1}_n^T Cp$ the distance becomes minimum, and substituting in (27) leads to

$$|x|_{\mathcal{A}}^2 = \left|(I - \frac{1}{n}\mathbb{1}_n\mathbb{1}_n^T)Cp\right|^2,$$

which is the desired result. □

Having these in view, we are ready to prove that the network achieves synchronization. In our system we are interested only in the synchronization of the voltage potentials p, hence we can view synchronization as stability of a suitable set $\mathcal{A}$, and make use of Theorem 12.

Theorem 15. *Consider the nonempty, closed, invariant set $\mathcal{A} \subset \mathbb{R}^{n+m}$, with $\mathcal{A} = \{x \in \mathbb{R}^{n+m} : p = b\mathbb{1}_n, b \in \mathbb{R}, \phi \in \mathbb{R}^m\}$. Then, a capacitor-memristor network, which is regarded as a simple, connected, undirected weighted graph and its dynamics are described by*

$$\begin{aligned} C\dot{p} &= -\mathcal{L}(\phi)p, \\ \dot{\phi} &= D^T p, \end{aligned} \tag{28}$$

is GAS with respect to set $\mathcal{A}$.

Proof. We define the function $V : \mathbb{R}^{n+m} \to \mathbb{R}_+$

$$V(x) = \frac{1}{2}|x|_{\mathcal{A}}^2 = \frac{1}{2}\left|(I - \frac{1}{n}\mathbb{1}\mathbb{1}^T)Cp\right|^2$$

as a Lyapunov function candidate of our system. In order for V to be a Lyapunov function for (28) with respect to the equilibrium set $\mathcal{A} \subset \mathbb{R}^{n+m}$ it has satisfy the two conditions of Definition 11. Let $\alpha_1(|x|_{\mathcal{A}}) = \frac{1}{2}|x|_{\mathcal{A}}^2$ and $\alpha_2(|x|_{\mathcal{A}}) = |x|_{\mathcal{A}}^2$ two $\mathcal{K}_\infty$-function, then for any $x \in \mathbb{R}^{n+m}$ it holds that

$$\frac{1}{2}|x|_{\mathcal{A}}^2 \leq \frac{1}{2}|x|_{\mathcal{A}}^2 \leq |x|_{\mathcal{A}}^2.$$

Thus, for the aforementioned functions α_1, α_2 the first condition is satisfied.

Next, we take the Lie derivative of V along trajectories of system (28) to obtain

$$\begin{aligned}\mathcal{L}_f V(x) &= \frac{\partial V}{\partial x}^T(x) f(x) \\ &= p^T(I - \frac{1}{n}\mathbb{1}_n\mathbb{1}_n^T)C\dot{p} \\ &= -p^T(I - \frac{1}{n}\mathbb{1}_n\mathbb{1}_n^T)\mathcal{L}(\phi)p \\ &= -p^T\mathcal{L}(\phi)p + p^T\frac{1}{n}\mathbb{1}_n\mathbb{1}_n^T\mathcal{L}(\phi)p.\end{aligned}$$

Recall the Laplacian property, that $\mathbb{1}_n^T\mathcal{L}(\phi) = 0$ if and only if the graph is connected (see Lemma 1). Using this the Lie derivative of V equals

$$\mathcal{L}_f V(x) = -p^T\mathcal{L}(\phi)p.$$

By Lemma 5, we can bound $\mathcal{L}_f V(x)$ as

$$\mathcal{L}_f V(x) = -\,p^T\mathcal{L}(\phi)p \leq -\frac{g_{min}\lambda_2(DD^T)}{n}p^T\mathcal{L}_{K_n}p$$

where g_{min} is a lower bound on $g(\phi)$, i.e. $g_{\text{min}} \leq g(\phi)$ for all $\phi \in \mathbb{R}^m$. Recall that $g(\phi)$ represents the memductances of the memristors, hence $g(\phi) > 0$ for all $\phi \in \mathbb{R}^m$ which implies that $g_{\text{min}} > 0$. Moreover, $\lambda_2(DD^T)$ denotes the second smallest eigenvalue of the matrix DD^T and consindering that the graph $\mathcal{G}$ is connected, the second eigenvalue of the Laplacian matrix DD^T is strictly positive.

Furthermore, substituting the Laplacian of the complete graph K_n from Lemma 2 yields

$$\mathcal{L}_f V(x) \leq -\frac{g_{min}\lambda_2(DD^T)}{n}p^T n(I - \frac{1}{n}\mathbb{1}_n\mathbb{1}_n^T)p. \tag{29}$$

We observe that $(I - \frac{1}{n}\mathbb{1}_n\mathbb{1}_n^T) = (I - \frac{1}{n}\mathbb{1}_n\mathbb{1}_n^T)(I - \frac{1}{n}\mathbb{1}_n\mathbb{1}_n^T)^T$. Next, as before the matrix C consists of the capacitance of each capacitor, therefore, C is a positive definite matrix. Additionally, it is true that there exist a positive constant $c > 0$ such that

$$p^T(I - \frac{1}{n}\mathbb{1}_n\mathbb{1}_n^T)p \geq c\left|(I - \frac{1}{n}\mathbb{1}_n\mathbb{1}_n^T)Cp\right|^2. \tag{30}$$

Multiplying inequality (30) by the negative value $-g_{\min}\lambda_2(DD^T)$ yields

$$-g_{\min}\lambda_2(DD^T)p^T(I-\frac{1}{n}\mathbb{1}_n\mathbb{1}_n^T)p \leq -g_{\min}\lambda_2(DD^T)c\left|(I-\frac{1}{n}\mathbb{1}_n\mathbb{1}_n^T)Cp\right|^2.$$

Hence, from (29) we can bound $\mathcal{L}_f V(x)$ as

$$\begin{aligned}\mathcal{L}_f V(x) \leq & -g_{min}\lambda_2(DD^T)c\left|(I-\frac{1}{n}\mathbb{1}_n\mathbb{1}_n^T)Cp\right|^2 \\ = & -g_{min}\lambda_2(DD^T)c\,|x|_{\mathcal{A}}^2.\end{aligned}$$

Let $\alpha_3(|x|_{\mathcal{A}}) = g_{min}\lambda_2(DD^T)c|x|_{\mathcal{A}}^2$, α_3 is a positive definite function for all $x \in \mathbb{R}^{n+m}\backslash\mathcal{A}$ since $g_{min}\lambda_2(DD^T)c > 0$, and satisfies the second condition of Definition 11, that is,

$$\mathcal{L}_f V(x) \leq -\alpha_3\left(|x|_{\mathcal{A}}\right).$$

It follows that $V(x) = \frac{1}{2}|x|_{\mathcal{A}}^2$ is a smooth Lyapunov function for the overall system, with respect to the set $\mathcal{A} = \{x \in \mathbb{R}^{n+m} \ : \ p = b\mathbb{1}_n, b \in \mathbb{R}, \phi \in \mathbb{R}^m\}$.

According to Lyapunov stability theory, and Theorem 12, the system (28) is GAS with respect to equilibrium set $\mathcal{A}$. Meaning that, the network consisting of memristors and capacitors, with different capacitance, will achieve synchronization. This completes the proof. □

5.3 Circuits with FHN neuron and memristor

In this section a different network is analyzed. We replace in the previous network the capacitors with FHN neurons and we provide a sufficient condition to guarantee synchronization.

5.3.1 Model description

Consider a network of FHN neurons coupled by memristor synapses. Based on Section 5.1 and similarly to memristors-capacitors network, we can model the dynamics with the use of a simple undirected, connected weighted graph $\mathcal{G}$ with n nodes and m edges.

In this case, instead of a capacitor in each node s we place a spiking neuron described by the two dimensional FitzHugh-Nagumo equation. The dynamics of an FHN neuron was analyzed in

Section 3.2.2 and is recalled as

$$\begin{aligned} \dot{p}_s &= p_s - \frac{1}{3}p_s^3 - w_s + j_s, \\ \dot{w}_s &= c(p_s + a - bw_s), \end{aligned} \tag{31}$$

where a, b, c are dimensionless parameters taking values between 0 and 1. The nodal current is denoted by j_s. Moreover, the state variables p_s and w_s stand for the voltage potential and the recovery variable, respectively.
As before, the dynamics of the k-th memristor is given by

$$\begin{aligned} \dot{\phi}_k &= v_k, \\ i_k &= G(\phi_k)v_k. \end{aligned}$$

Hence, if we denote $x = \begin{pmatrix} p & w & \phi \end{pmatrix},^T$ a FHN neuron - memristor network can be described by a time-invariant and forward complete system $\dot{x} = f(x)$ as

$$\begin{aligned} \dot{p} &= p - \frac{1}{3}\psi(p) - w - \mathcal{L}(\phi)p, \\ \dot{w} &= c(p + a\mathbb{1}_n - bw), \\ \dot{\phi} &= D^T p, \end{aligned} \tag{32}$$

where as $\mathcal{L}(\phi) = DG(\phi)D^T$ and by $\psi(p)$ we denote the vector $\psi(p) = \begin{pmatrix} p_1^3 & p_2^3 & \dots & p_n^3 \end{pmatrix}^T$.

5.3.2 Proof of synchronization

In this subsection, we will follow a Lyapunov stability approach in order to investigate the conditions for synchronization of a FHN neuron - memristor network.

We denote the state variables of the system (32) by the vector $x = \begin{pmatrix} p & w & \phi \end{pmatrix}^T \in \mathbb{R}^{2n+m}$. Consider the nonempty, closed, invariant set $\mathcal{A} \subseteq \mathbb{R}^{2n+m}$

$$\mathcal{A} = \{x \in \mathbb{R}^{2n+m} : p = k\mathbb{1}_n, w = l\mathbb{1}_n, k, l \in \mathbb{R}, \phi \in \mathbb{R}^m\}.$$

For stability analysis, as for the capacitors case, we are interested in the synchronization of the voltage potentials, therefore we will use the GAS with respect to an invariant set approach. Hence, it is necessary first to establish the distance function between a point $x \in \mathbb{R}^{2n+m}$ and the set $\mathcal{A}$.

Lemma 16. *Consider the vector* $x = \begin{pmatrix} p & w & \phi \end{pmatrix}^T \in \mathbb{R}^{2n+m}$. *Let the nonempty, closed, invariant set* $\mathcal{A} \subseteq \mathbb{R}^{2n+m}$, *with* $\mathcal{A} = \{x \in \mathbb{R}^{2n+m} : p = k\mathbb{1}_n, w = l\mathbb{1}_n, k, l \in \mathbb{R}, \phi \in \mathbb{R}^m\}$. *Then the distance between a point* $x \in \mathbb{R}^{2n+m}$ *and the set* $\mathcal{A}$ *is equal to*

$$|x|_{\mathcal{A}}^2 = \left|(I - \frac{1}{n}\mathbb{1}_n\mathbb{1}_n^T)p\right|^2 + \left|(I - \frac{1}{n}\mathbb{1}_n\mathbb{1}_n^T)w\right|^2.$$

Proof. The distance between any point $x = \begin{pmatrix} p & w & \phi \end{pmatrix}^T \in \mathbb{R}^{2n+m}$ and the non-empty set $\mathcal{A}$ is given by

$$|x|_{\mathcal{A}}^2 = d(x, \mathcal{A})^2 = \inf_{\eta \in \mathcal{A}} d(x, \eta)^2 = \inf_{\eta \in \mathcal{A}} \left| \begin{pmatrix} p \\ w \\ \phi \end{pmatrix} - \eta \right|.^2$$

Using the definition of set $\mathcal{A}$ yields

$$|x|_{\mathcal{A}}^2 = \inf_{k,l \in \mathbb{R}} \left| \begin{pmatrix} p \\ w \\ \phi \end{pmatrix} - \begin{pmatrix} k\mathbb{1}_n \\ l\mathbb{1}_n \\ \phi \end{pmatrix} \right|^2 = \inf_{k,l \in \mathbb{R}} \left| \begin{pmatrix} p - k\mathbb{1}_n \\ w - l\mathbb{1}_n \end{pmatrix} \right|^2. \tag{33}$$

In order to find the $k, l \in \mathbb{R}$ that minimize the above distance we take a least square approach. Multiplying by $\mathbb{1}_n^T$ yields

$$k^*\mathbb{1}_n^T\mathbb{1}_n = \mathbb{1}_n^T p \implies k^* = \frac{1}{n}\mathbb{1}_n^T p,$$

similarly,

$$l^*\mathbb{1}_n^T\mathbb{1}_n = \mathbb{1}_n^T w \implies l^* = \frac{1}{n}\mathbb{1}_n^T w.$$

Hence, substituting the k^*, l^* back into (33) we obtain the desired distance

$$|x|_{\mathcal{A}}^2 = \left|(I - \frac{1}{n}\mathbb{1}_n\mathbb{1}_n^T)p\right|^2 + \left|(I - \frac{1}{n}\mathbb{1}_n\mathbb{1}_n^T)w\right|^2.$$

□

Having these in mind we are in position to state and prove that FHN neurons coupling via memristors achieve synchronization. We will obtain this result based on Theorem 13.

Theorem 17. *Consider an FHN neuron -memristor network which is regarded as a simple, connected, undirected weighted graph* $\mathcal{G}$ *and its dynamics are described by* (32). *Then, system* (32)

is GAS with respect to the nonempty, closed, invariant set $\mathcal{A} = \{x \in \mathbb{R}^{2n+m} : p = k\mathbb{1}_n, w = l\mathbb{1}_n, k, l \in \mathbb{R}, \phi \in \mathbb{R}^m\}$ *if for all* $\phi \in \mathbb{R}^m$ *the memductance* $g(\phi)$ *satisfies the following condition*

$$g(\phi) > \frac{1}{\lambda_2(DD^T)},$$

where $\lambda_2(DD^T)$ *is the second smallest eigenvalue of the Laplacian matrix* DD^T *of the graph* $\mathcal{G}$.

Proof. Let $x = \begin{pmatrix} p & w & \phi \end{pmatrix}^T \in \mathbb{R}^{2n+m}$, and define the function $V : \mathbb{R}^{2n+m} \to \mathbb{R}_+$ given by

$$V(x) = \frac{1}{2n}\left|n(I - \frac{1}{n}\mathbb{1}_n\mathbb{1}_n^T)p\right|^2 + \frac{1}{2nc}\left|n(I - \frac{1}{n}\mathbb{1}_n\mathbb{1}_n^T)w\right|^2$$

as a Lyapunov function candidate for the system (32).

We define the $\mathcal{K}_\infty$-functions $\alpha_1(|x|)_\mathcal{A} = \frac{1}{2}n|x|_\mathcal{A}^2$ and $\alpha_2(|x|)_\mathcal{A} = \frac{1}{2c}n|x|_\mathcal{A}^2$, for which it holds that

$$\frac{1}{2}n|x|_\mathcal{A}^2 \leq \frac{1}{2n}\left|n(I - \frac{1}{n}\mathbb{1}_n\mathbb{1}_n^T)p\right|^2 + \frac{1}{2nc}\left|n(I - \frac{1}{n}\mathbb{1}_n\mathbb{1}_n^T)w\right|^2 \leq \frac{1}{2c}n|x|_\mathcal{A}^2.$$

Hence, the first condition of Definition 11 is satisfied.

By Lemma 2, we can denote $n(I - \frac{1}{n}\mathbb{1}_n\mathbb{1}_n^T) = \mathcal{L}_{K_n}$, hence, the Lyapunov function candidate can be written as,

$$V(x) = \frac{1}{2n}\left|\mathcal{L}_{K_n}p\right|^2 + \frac{1}{2nc}\left|\mathcal{L}_{K_n}w\right|^2. \tag{34}$$

Next, the time derivative of (34) along the trajectories of system (32) yields

$$\begin{aligned}
\mathcal{L}_f V(x) =& \frac{\partial V^T}{\partial x}(x)f(x) \\
=& \frac{1}{n}p^T n\mathcal{L}_{K_n}\dot{p} + \frac{1}{nc}w^T n\mathcal{L}_{K_n}\dot{w} \\
=& p^T\mathcal{L}_{K_n}\left(p - \frac{\psi(p)}{3} - w - \mathcal{L}(\phi)p\right) + \frac{1}{c}w^T\mathcal{L}_{K_n}c\left(p + a\mathbb{1}_n - bw\right) \\
=& p^T\mathcal{L}_{K_n}p - p^T\mathcal{L}_{K_n}\frac{\psi(p)}{3} - p^T\mathcal{L}_{K_n}\mathcal{L}(\phi)p - p^T\mathcal{L}_{K_n}w + w^T\mathcal{L}_{K_n}p + w^T\mathcal{L}_{K_n}(a\mathbb{1}_n) - bw^T\mathcal{L}_{K_n}w.
\end{aligned} \tag{35}$$

We can simplify equation (35) using the Laplacian properties from Lemma 1.

Due to symmetry of the Laplacian matrix,

$$p^T \mathcal{L}_{K_n} w = w^T \mathcal{L}_{K_n} p.$$

In addition, we have that

$$w^T \mathcal{L}_{K_n}(a\mathbb{1}_n) = a(w^T \mathcal{L}_{K_n} \mathbb{1}_n) = 0,$$

and, lastly, the quantity $p^T \mathcal{L}_{K_n} \mathcal{L}(\phi) p$ can be written as

$$p^T \mathcal{L}_{K_n} \mathcal{L}(\phi) p = p^T n(I - \frac{1}{n}\mathbb{1}_n \mathbb{1}_n^T)\mathcal{L}(\phi) p = np^T \mathcal{L}(\phi) p.$$

Thus, expression (35) becomes

$$\mathcal{L}_f V(x) = p^T \mathcal{L}_{K_n} p - p^T \mathcal{L}_{K_n} \frac{\psi(p)}{3} - np^T \mathcal{L}(\phi) p - bw^T \mathcal{L}_{K_n} w.$$

Recall that $\psi(p) = \begin{pmatrix} p_1^3 & p_2^3 & \dots p_n^3 \end{pmatrix}^T$ we can apply Lemma 3, on $p^T \mathcal{L}_{K_n} \frac{1}{3}\psi(p)$ to obtain

$$p^T \mathcal{L}_{K_n} \frac{\psi(p)}{3} = \sum_{\{i,j\} \in \mathcal{E}}^{n} (p_i - p_j) \left(\frac{p_i^3}{3} - \frac{p_j^3}{3} \right).$$

For any $p \in \mathbb{R}^n$, both terms in parenthesis have the same sign, therefore $p^T \mathcal{L}_{K_n} \frac{\psi(p)}{3} \geq 0$. As result, we can set an upper bound for $\mathcal{L}_f V(x)$ as

$$\mathcal{L}_f V(x) \leq p^T \mathcal{L}_{K_n} p - np^T \mathcal{L}(\phi) p - bw^T \mathcal{L}_{K_n} w. \tag{36}$$

By Lemma 5 ,

$$np^T \mathcal{L}(\phi) p \geq g_{min} \lambda_2(DD^T) p^T \mathcal{L}_{K_n} p$$

where g_{min} represents the lower bound of the memductance $g(\phi)$. Hence, (36) can be written as

$$\begin{aligned} \mathcal{L}_f V(x) &\leq p^T \mathcal{L}_{K_n} p - g_{min} \lambda_2(DD^T) p^T \mathcal{L}_{K_n} p - bw^T \mathcal{L}_{K_n} w \\ &= \left(1 - g_{min} \lambda_2(DD^T)\right) p^T \mathcal{L}_{K_n} p - bw^T \mathcal{L}_{K_n} w \end{aligned} \tag{37}$$

From the definition of $\mathcal{L}_{K_n}$ holds that $\mathcal{L}_{K_n} = \frac{1}{n}\mathcal{L}_{K_n}\mathcal{L}_{K_n}^T$ since

$$n(I - \frac{1}{n}\mathbb{1}_n \mathbb{1}_n^T) = \frac{1}{n} n(I - \frac{1}{n}\mathbb{1}_n \mathbb{1}_n^T) n(I - \frac{1}{n}\mathbb{1}_n \mathbb{1}_n^T)^T.$$

Substituting $\mathcal{L}_{K_n}$ in (37) we obtain

$$\begin{aligned}\mathcal{L}_f V(x) &\leq \left(1 - g_{min}\lambda_2(DD^T)\right)\frac{1}{n}\left|\mathcal{L}_{K_n}p\right|^2 - \frac{1}{n}b\left|\mathcal{L}_{K_n}w\right|^2 \\ &= n\left(1 - g_{min}\lambda_2(DD^T)\right)\left|\left(I - \frac{1}{n}\mathbb{1}_n\mathbb{1}_n^T\right)p\right|^2 - nb\left|\left(I - \frac{1}{n}\mathbb{1}_n\mathbb{1}_n^T\right)w\right|^2.\end{aligned} \tag{38}$$

In order to have synchronization of system (32) the Lyapunov functionn candidate must satisfy the second condition of Definition 11, meaning that should exists a positive function $\alpha_3(|x)|_{\mathcal{A}}$ such that

$$\mathcal{L}_f V(x) \leq -\alpha_3(|x|)_{\mathcal{A}}, \text{ for all } x \in \mathbb{R}^{2n+m}\backslash\mathcal{A}.$$

Given the connectivity of the graph, $\lambda_2(DD^T) > 0$, therefore if

$$g_{min} > \frac{1}{\lambda_2(DD^T)}, \tag{39}$$

then inequality (38) can be bounded by

$$\mathcal{L}_f V(x) \leq -\mu\left(\left|\left(I - \frac{1}{n}\mathbb{1}_n\mathbb{1}_n^T\right)p\right|^2 + \left|\left(I - \frac{1}{n}\mathbb{1}_n\mathbb{1}_n^T\right)w\right|^2\right),$$

where μ is a positive constant which is guaranteed to exist if condition (39) holds. Thus, for $\alpha_3(|x|)_{\mathcal{A}} = \mu|x|^2_{\mathcal{A}}$, we have proved the statement, and $V(x)$ is a smooth Lyapunov function with respect to set $\mathcal{A}$ for the system (32).

According to Theorem 12, system (32) is GAS with respect to set $\mathcal{A}$ under the assumption that for all $\phi \in \mathbb{R}^m$, the memductance $g(\phi)$ is lower bounded by

$$g(\phi) > \frac{1}{\lambda_2(DD^T)}. \tag{40}$$

□

The previous result states that if the memductance of the memristive devices is sufficiently high, then the memristance is low and synchronization can be achieved. Nevertheless, the above theorem provides only a sufficient, but not a necessary condition for synchronization of the circuit. Namely, if the memductance does not satisfy the inequality (40) , the condition does not imply that the circuit cannot be synchronized.

6 Simulations

In this chapter, simulation results are presented to illustrate the aforementioned theoretical results and further explore the dynamics of electrical circuits with memristors.

For the numerical results we proposed a two-terminal, time-invariant flux-controlled memristor which is described by the equations

$$\begin{aligned}\dot{\phi}(t) &= v(t),\\ i(t) &= (d_1 \arctan(\phi) + d_2)v(t).\end{aligned}$$

Correspondingly, the device's memductance is represented by the function $g(\phi) = d_1 \arctan(\phi) + d_2$, and the parameters $d_1, d_2 \geq 0$ stand for the coupling coefficients. Moreover, we choose $d_2 > d_1$ to ensure that $g(\phi) > 0$ for all ϕ.
Notice that when $d_1 = 0$, the memductance is of the form $g(\phi) = d_2$, and the memristor model reduces to a linear resistor.

6.1 Circuits with capacitors and memristors.

In this section, we present simulation results to verify the synchronization of the memristors-capacitors network as shown in Theorem 15.

As derived in Section 5.2, the network of n capacitors and m memristors can be described as

$$\begin{aligned}C\dot{p} &= -DG(\phi)D^T p,\\ \dot{\phi} &= D^T p,\end{aligned}$$

where $C \in \mathbb{R}^{n\times n}$ is a diagonal matrix having as elements the capacitance of the capacitors. The matrix $G(\phi) = \text{diag}\{g(\phi_i)\}_{i=1}^m = \text{diag}\{d_1 \arctan(\phi_i) + d_2\}_{i=1}^m$ has the memductances of the proposed memristor as entries, and D is the incidence matrix that describes the network structure.

At the beginning, we investigate the dynamic behaviour of the electrical network of two identical capacitors with capacitance $c_1 = c_2 = 3$, coupled with the proposed memristor as shown in Figure 14. We set the initial conditions as $p_0 = (1.5, 0.6)$ and $\phi_0 = -0.4$.

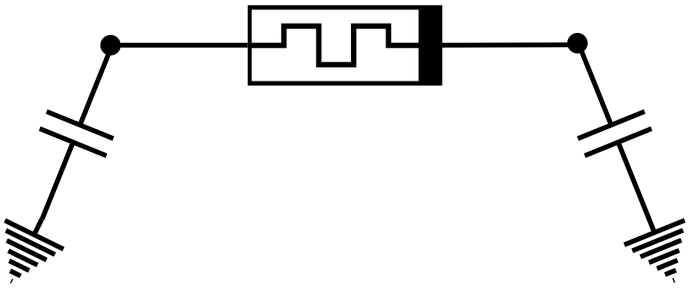

Figure 14: Schematic diagram of an electrical network consisting of 2 capacitors and 1 memristor.

Initially, we fix the first coefficient of the memductance equal to zero, i.e., $d_1 = 0$, and the second as $d_2 = 0.2$. In this case, the memristor reduces to a linear resistor. In the next simulation, the second coefficient remains as $d_2 = 0.2$, while we set the first coefficient as $d_1 = 0.1$. As illustrated in Figure 15 in both cases the network is driven to synchronization. However, the network with the resistor has a slower convergence rate than the memristor network, see Figure $15b$.

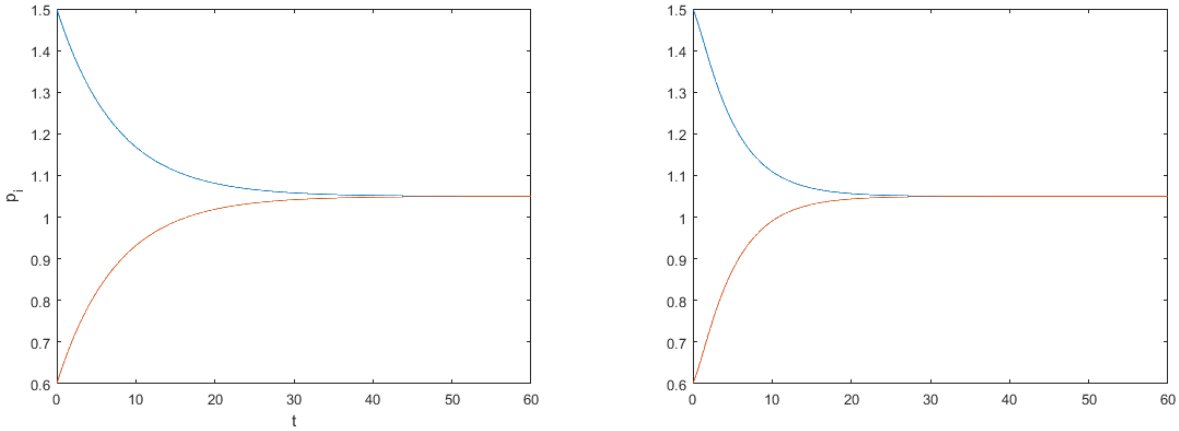

(a) $d_1 = 0$ and $d_2 = 0.2$

(b) $d_1 = 0.1$ and $d_2 = 0.2$

Figure 15: Trajectories of the voltage potentials p_i of two capacitors coupled with one memristor with memductance $g(\phi) = d_1 \arctan(\phi) + d_2$.

Hence, in this case the proposed memristor contributes to the dynamics of the network and provides faster synchronization.

This result can be verified by looking at the evolution of the memristor memductance value $g(\phi)$. As illustrated in Figure 16 the value of the memductance for $d_1 = 0.1$ is larger than for the linear resistor, i.e., $d_1 = 0$, on average.

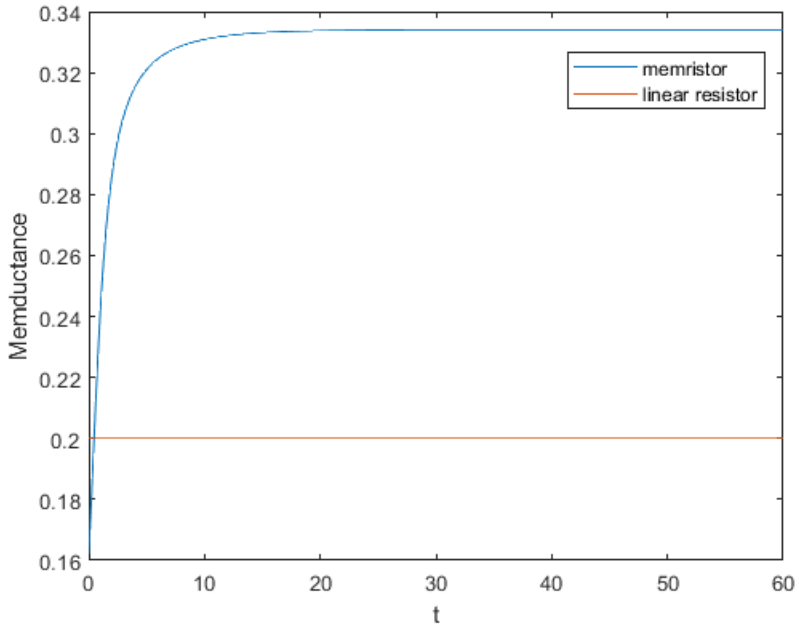

Figure 16: Time evolution of memductances for the memristor and the linear resistor. The blue curve corresponds to the memristor with memductance $g(\phi) = 0.1 \arctan(\phi) + 0.2$, while the straight line corresponds to a linear resistor with memductance $g(\phi) = 0.2$.

Next, we analyze the dynamic behaviour of a more complicated network.

Consider the electrical network in Figure 17 consisting of 5 memristors coupled with 4 capacitors connected to ground. The initial state of the network and the capacitance of each capacitor are fixed as $p_0 = (3.1, -2.2, 0.5, 3.6)$, $\phi_0 = (0.3, 0.5, 0.7, 0.1, 0.5)$ and $C = \text{diag}\,(2, 1, 6, 3)$.

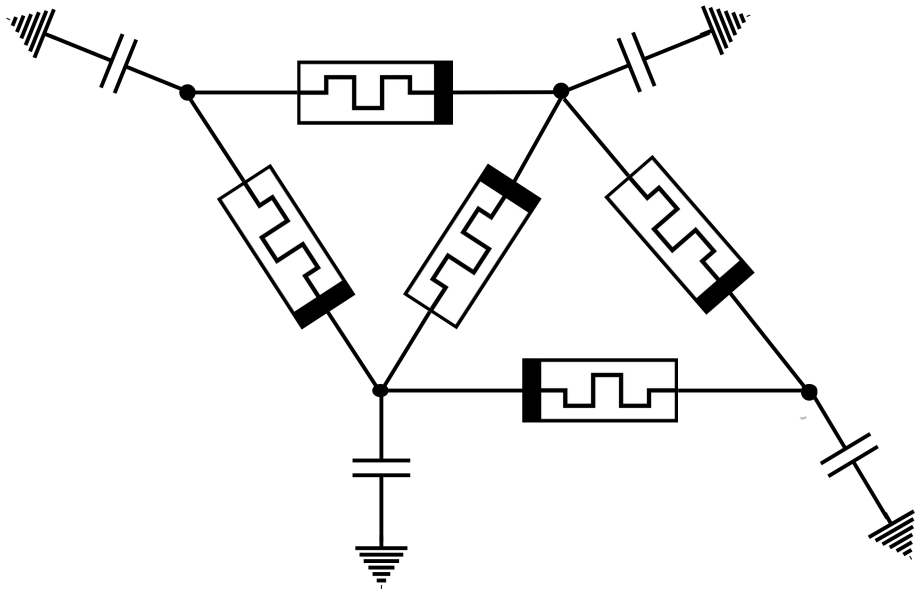

Figure 17: Schematic diagram of electrical network consisting of 4 capacitors and 5 memristors.

First, we set the memristor coupling coefficients as $d_1 = 0.2$ and $d_2 = 0.5$. As illustrated in Figure $18a$, the voltage potentials $p_i(t)$ are synchronized and remain in a steady state solution. Furthermore, each of the flux-linkages of the memristors converge to a steady-state value as well, as shown in Figure $18b$.

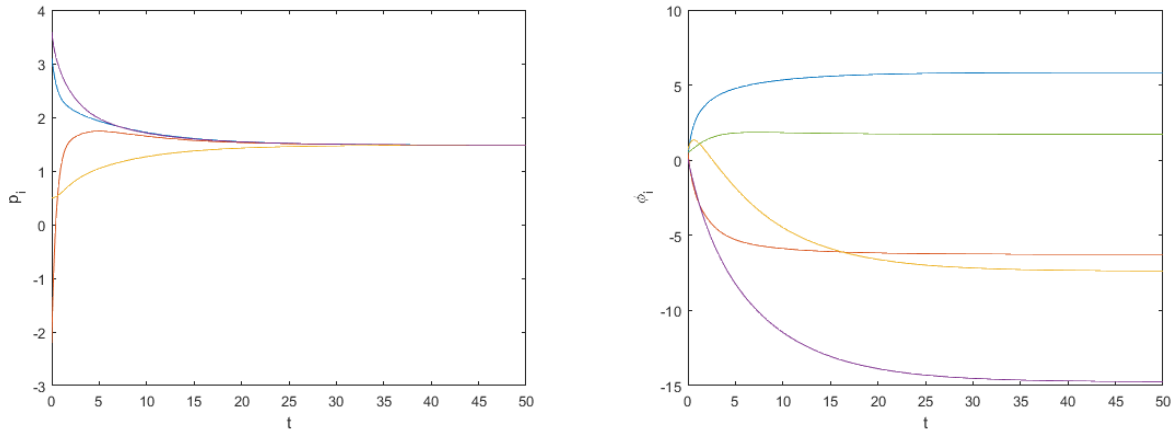

(a) Trajectory of the voltage potential.

(b) Trajectrory of the flux-linkage.

Figure 18: the state variables of the network depicted in Figure 17. Here the memductance is $g(\phi) = 0.2\arctan(\phi) + 0.5$.

Next, the first coupling coefficient is kept as $d_1 = 0.2$, whereas the second coefficient of the memductance is changed. As depicted in Figure 19 the voltage potentials are driven to synchronization

much faster for increasing values of d_2, see Figure 19. This is an interesting observation since this implies that higher memductance values lead to a faster convergence towards the consensus of the voltage potentials.

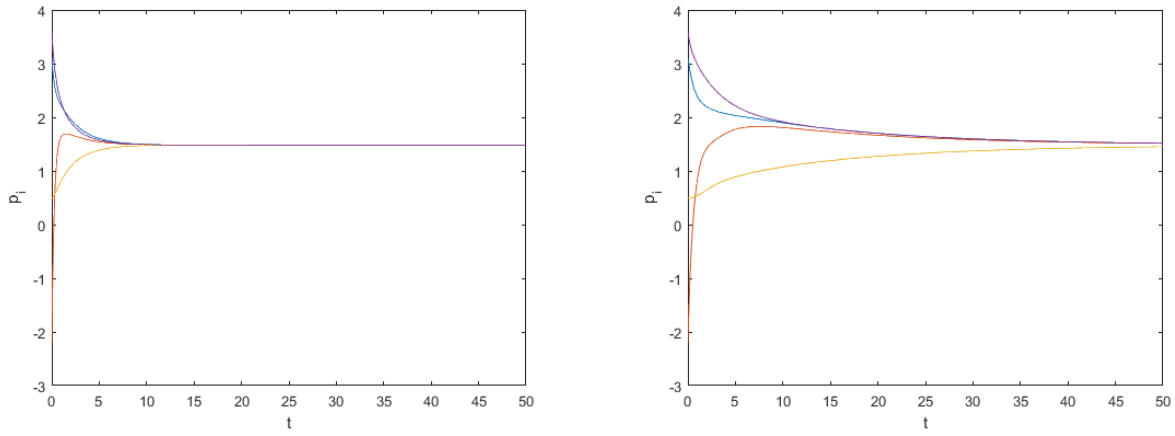

(a) $d_1 = 0.2$ and $d_2 = 1$ (b) $d_1 = 0.2$ and $d_2 = 0.4$

Figure 19: Trajectories of the voltage potentials of the network depicted in Figure 17 with memductance $g(\phi) = d_1 \arctan(\phi) + d_2$.

6.2 Networks with FHN neurons and memristors.

In this section, we demonstrate the synchronization property and we study the influence of the memristors-FHN neuron networks.

Consider the network of two identical FHN neurons coupled via a memristor synapse shown in Figure 20. As specified in Section 5.3, the dynamics of the networks is described as

$$\begin{aligned}
\dot{p_1} &= p_1 - \frac{p_1}{3} - w_1 + I_{ext} - (d_1 \arctan(\phi) + d_2)(p_1 - p_2),\\
\dot{p_2} &= p_2 - \frac{p_2}{3} - w_2 + I_{ext} + (d_1 \arctan(\phi) + d_2)(p_1 - p_2),\\
\dot{w_1} &= c(p_1 + a - bw_1),\\
\dot{w_2} &= c(p_2 + a - bw_2),\\
\dot{\phi} &= p_1 - p_2.
\end{aligned}$$

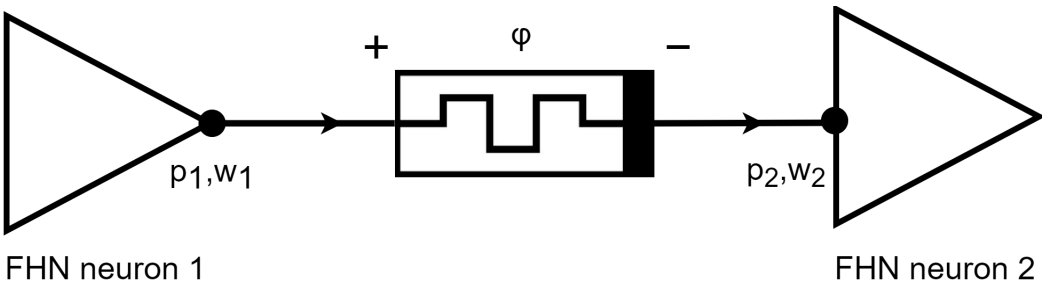

Figure 20: Schematic diagram of two FHN neurons coupled via a memristor.

In all cases parameters values are chosen as $a = 0.7, b = 0.8, c = 0.08, I_{ext} = 0.6$ and initial conditions as $p_0 = (1.6, 2.1)$, $w_0 = (0.3, 1.4)$ and $\phi_0 = 1.5$. Both the memristor coupling coefficients d_1 and d_2 are adjustable.

First, we fixed the memristor coupling terms as $d_1 = 0.2$ and $d_2 = 0.5$. As depicted in Figure 21 the membrane potentials $p_i(t)$ of the neurons synchronize to a common harmonic oscillation. In a similar way the two recovery variables w_i become synchronized.

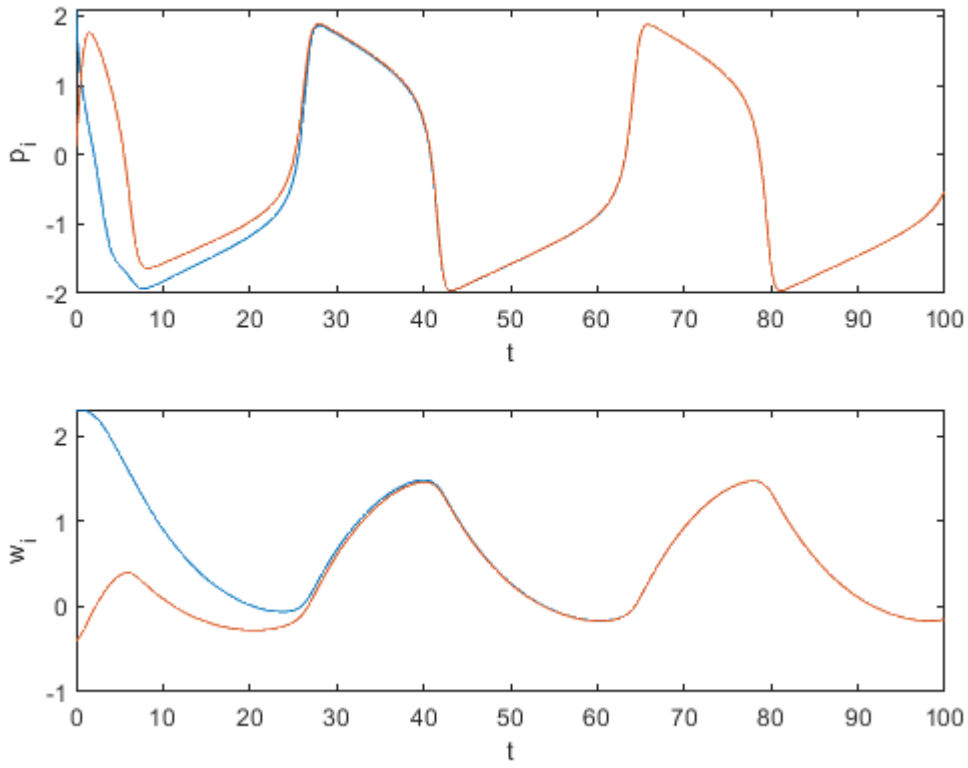

Figure 21: Trajectories of the state variables p_i, w_i of two coupled FHN neurons via a memristor with memductance $g(\phi) = 0.1 \arctan(\phi) + 0.5$.

Next, the two coupling coefficients of the memristor are set as $d_1 = 0.01$, $d_2 = 0.02$, whereas the initial state remains the same. The results shown in Figure 22 demonstrate that the system still tends to be completely synchronized, but that the convergence rate is much slower.

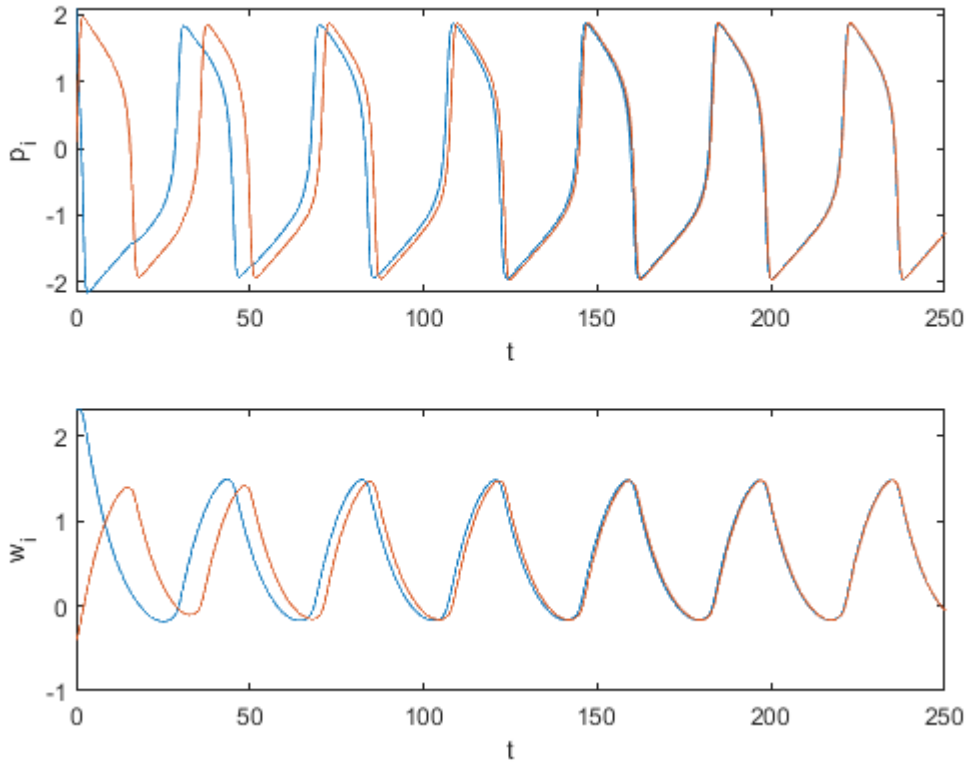

Figure 22: Trajectories of the state variables p_i, w_i of two coupled FHN neurons via a memristor with memductance $g(\phi) = 0.01 \arctan(\phi) + 0.02$.

Thus, the coupling coefficients of the memristors have an influence on the synchronization of the neuron network, but with the passage of time, the system ultimately results in a complete synchronization mode. This result can be related to the sufficient condition of Theorem 17 which states that in order to guarantee synchronization of the voltage potentials, the memductance should be lower bounded by the given value.

Finally, in order to conclude on the generality of Theorem 17, a more advanced memristor-FHN neuron network is considered. We choose a circuit consisting of 6 FHN-neuron models coupled via 8 memristors as depicted in Figure 23.

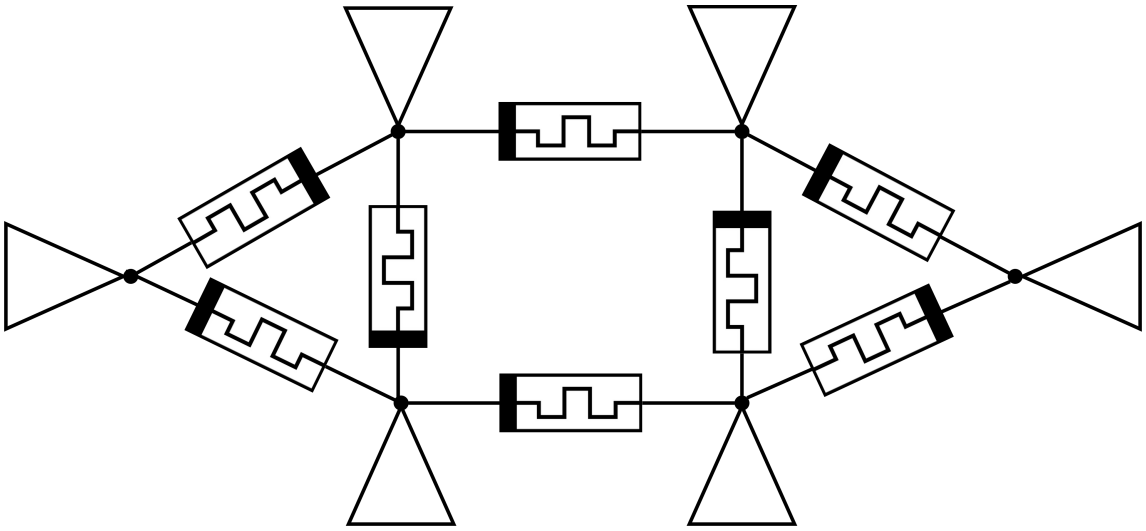

Figure 23: Schematic diagram of 6 FHN neurons coupled via 8 memristors.

The initial state of the network is $p_0 = (2.1, 2.4, -0.2, -0.5, 0.6, 0.8)$, $w_0 = (1.4, 0.1, 2.3, -0.4, 0.1, 0.4)$ and $\phi_0 = (-0.6, 0.3, 0.7, -0.6, 0.07, 0.9, -2.1, -0.05)$, while the FHN neuron parameters remain as $a = 0.7, b = 0.8, c = 0.08, I_{ext} = 0.6$ and the coupling coefficients of the memristors are $d_1 = 0.1$ and $d_2 = 0.2$.

As it was expected, Figure 24 depicts that, even though the dynamics is more complex in comparison with two coupled FHN neurons, the voltage potentials as well as the recovery variables become synchronized.

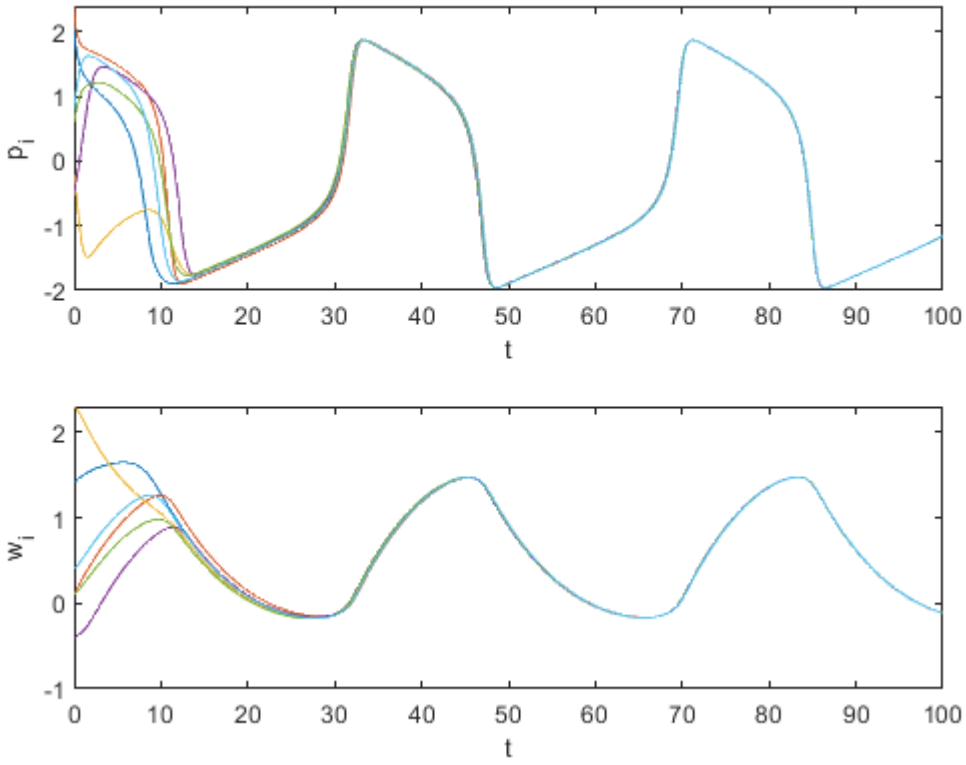

Figure 24: Trajectories of the state variables p_i, w_i of the network depicted in Figure 23.

7 Conclusion

This work can provide a further theoretical understanding of the behaviour of memristors coupled with different electrical elements, and their potential applications as building blocks for neuromorphic computing architectures.

Firstly, we introduced memristors and we laid out their most relevant properties. Thereafter, the first physical model of the memristor was presented. Then, in order to study if the memristor could be used as a synapse for transmitting information between interconnected neurons, we briefly explained how biological neural networks communicate through synapses and how action potential is generated. In this sense, two of the most well-known neuron models, the Hodgkin-Huxley and the FitzHugh-Nagumo, were discussed.

Subsequently, we modelled electrical circuits consisting of memristors and capacitors. This is realized by describing these circuits as simple, undirected, weighted graphs, whose edges correspond to the memristors, and whose nodes correspond to the capacitors. Thereafter, we used Lyapunov stability reasoning and global asymptotic stability with respect to an invariant set, in order to prove that the capacitor-memristor networks achieve synchronization. Similarly, electrical circuits, which simulate the dynamic behaviour of the FHN neuron models coupled via memristors were designed, and a sufficient condition of synchronization was derived. In a brain, neuronal activity is synchronized, to process and transfer information. Consequently, we showed that electrical circuits of memristive elements can achieve synchronization, therefore the memristor could be possibly used as a building block for simulating artificial synapses.

Finally, in the simulation results section, a flux-controlled memristor model was adopted and used as a coupling element between electronic circuits. We saw that electrical circuits reach synchronization, despite the initial conditions and the coupling factors of the memristor. Nevertheless, we observe that the parameters values of the memristor influence the convergence rate of the system, meaning that higher values of memductance increase the rate of synchronization.

An interesting direction of future work is to broaden these results in memristive devices, since most practical devices are memristive systems. For example, we can replace the memristor model by a broaden spectrum of memristive models and then investigate if these circuits achieve synchronization. Furthermore, adding external input to the memristor - FHN neuron circuits is another promising direction. The human brain processes information and the addition of an external input in the aforementioned model provides a first step in modeling and analyzing this circuit. Prov-

ing that the circuit is input-to-state convergent will demonstrate many desired stability properties. Following that, we would like to study not only the synchronization behaviour of the voltage potentials, but we also want to gain more insight in the behaviour of the memristors themselves. Lastly, in any realistic application, noise is expected to affect the performance of memristor circuits. For instance, if the circuit does not synchronize under the influence of noise, memristors may not be suitable to simulate synapses.

References

[1] G. E. Moore. Cramming more components onto integrated circuits. *Proceedings of the IEEE*, 86(1):82–85, 1998.

[2] T. N. Theis and H. . P. Wong. The end of moore's law: A new beginning for information technology. *Computing in Science Engineering*, 19(2):41–50, 2017.

[3] D. J. Frank, R. H. Dennard, E. Nowak, P. M. Solomon, Y. Taur, and Hon-Sum Philip Wong. Device scaling limits of si mosfets and their application dependencies. *Proceedings of the IEEE*, 89(3):259–288, 2001.

[4] Bernabe Linares-Barranco, Teresa Serrano-Gotarredona, Luis Camuñas-Mesa, Jose Perez-Carrasco, Carlos Zamarreño-Ramos, and Timothee Masquelier. On spike-timing-dependent-plasticity, memristive devices, and building a self-learning visual cortex. *Frontiers in Neuroscience*, 5:26, 2011.

[5] Yibo Li, Zhongrui Wang, Rivu Midya, Qiangfei Xia, and J Joshua Yang. Review of memristor devices in neuromorphic computing: materials sciences and device challenges. *Journal of Physics D: Applied Physics*, 51(50):503002, sep 2018.

[6] Andy Thomas. Memristor-based neural networks. *Journal of Physics D: Applied Physics*, 46:093001, 02 2013.

[7] L. Chua. Memristor-the missing circuit element. *IEEE Transactions on Circuit Theory*, 18(5):507–519, 1971.

[8] The Editors of Encyclopaedia Britannica. *Memristor*, October 07, 2020. `https://www.britannica.com/technology/memristor`.

[9] L. O. Chua and Sung Mo Kang. Memristive devices and systems. *Proceedings of the IEEE*, 64(2):209–223, 1976.

[10] Francesco Caravelli and Juan Pablo Carbajal. Memristors for the curious outsiders. *CoRR*, abs/1812.03389, 2018.

[11] Dmitri Strukov, Gregory Snider, Duncan Stewart, and Stan Williams. The missing memristor found. *Nature*, 453:80–3, 06 2008.

[12] E.M. Izhikevich. *Dynamical Systems in Neuroscience*. Computational neuroscience Dynamical systems in neuroscience. MIT Press, 2007.

[13] Wulfram Gerstner, Werner M. Kistler, Richard Naud, and Liam Paninski. *Neuronal Dynamics: From Single Neurons to Networks and Models of Cognition*. Cambridge University Press, 2014.

[14] The university of Queensland. Action potentials and synapses, 2017. `https://qbi.uq.edu.au/brain-basics/brain/brain-physiology/action-potentials-and-synapses`.

[15] A.F. Hodgkin, A.L. Huxley. A quantitative description of membrane current and its application to conduction and excitation in nerve. *Journal of Physiology (Lond.)*, 117(4):500–544., August 1952.

[16] Safa Yaghini Bonabi, Hassan Asgharian, Saeed Safari, and Majid Nili Ahmadabadi. FPGA implementation of a biological neural network based on the hodgkin-huxley neuron model. *Frontiers in Neuroscience*, 8:379, 2014.

[17] Richard FitzHugh. Impulses and physiological states in theoretical models of nerve membrane. *Biophysical Journal*, 1(6):445 – 466, 1961.

[18] Arimoto S.; Yoshizawa S. Nagumo, J. An active pulse transmission line simulating nerve axon. *Proc. IRE*, 50(10):2061–2070, October 1962.

[19] F. Bullo. *Lectures on Network Systems*. Kindle Direct Publishing, 2019. With contributions by J. Cortes, F. Dorfler, and S. Martinez.

[20] Bollobás Béla. *Modern Graph Theory*. Graduate Texts in Mathematics 184. Springer-Verlag New York, 1998.

[21] Mehran Mesbahi and Magnus Egerstedt. *Graph Theoretic Methods in Multiagent Networks*. Princeton University Press, stu - student edition edition, 2010.

[22] Roger A. Horn and Charles R. Johnson. *Matrix Analysis*. Cambridge University Press, 1985.

[23] A. Pavlov, N. Wouw, van de, and H. Nijmeijer. *Uniform output regulation of nonlinear systems : a convergent dynamics approach*. Systems and control : foundations and applications. Birkhäuser Verlag, Switzerland, 2006.

[24] Arjan van der Schaft and Jacquelien Scherpen. *Lecture notes Modeling and Control of Complex Nonlinear Engineering Systems*. 2018.

[25] Hassan K. Khalil. *Nonlinear Systems*. Prentice Hall, 3 edition, 1998.

[26] Eduardo D. Sontag Yuandan Lin and Yuan Wang. A smooth converse lyapunov theorem for robust stability. *SIAM J. Control Optim.*, 34(1):124–160., January 1996.

[27] Charles A. Desoer and Ernest S. Kuh. *Basic circuit theory*. McGraw-Hill New York, 1969.

[28] J. Willems. Terminals and ports. *IEEE Circuits and Systems Magazine*, 10:8–26, 2010.